Mapping Non-Syndromic Hearing Impairment Genes

A thesis submitted in partial fulfillment of the requirements for the degree of

Master of Philosophy in

Biochemistry/ Molecular Biology

by

Zia ur Rehman

Department of Biochemistry
Faculty of Biological Sciences
Quaid-i-Azam University
Islamabad
2008

DECLARATION

I hereby declare that the work presented in the following thesis is my own effort, except where otherwise acknowledged, and that the thesis is my own composition. No part of the thesis has been previously presented for any other degree.

Zia ur Rehman

Certificate

This thesis by **Mr. Zia ur Rehman** is accepted in its present form by the Department of Biochemistry, Quaid-i-Azam University, Islamabad, as fulfilling the thesis requirement for the degree of Master of Philosophy in Biochemistry/Molecular Biology.

Internal Examiner:

Prof. Dr. Wasim Ahmad

External Examiner:

Dr. Allah Nawaz

Chairman:

Prof. Dr. Wasim Ahmad

Dated: 14/03/2008

DEDICATED

TO

MY CUTE AND SWEET NEPHEWS

'NAVEED' AND 'JUNAID'

CONTENTS

	Page No.
ACKNOWLEDGEMENTS	I
LIST OF TABLES	II
LIST OF FIGURES	III
LIST OF ABBREVIATIONS	XI
ABSTRACT	XIV
INTRODUCTION	1
▪ Mechanism of Hearing	2
▪ Types of Hearing Loss	3
▪ Degree of Hearing Loss	3
▪ Causes of Hearing loss	4
▪ Environmental Causes	4
▪ Genetic or Heritable causes	4
▪ Syndromic Hearing impairment	5
▪ Non-Syndromic Hearing loss	5
▪ Genes Implicated in Hearing Loss	6
▪ GJB2 (Connexin 26)	6
▪ GJB6 (Connexin 30)	7
▪ GJB3 (Connexin 31)	7
▪ MYO7A (Myosin VIIA) - DFNB2	7
▪ MYO15 (Myosin XV) – DFNB3	8
▪ SLC26A4 (Pendrin) – DFNB4	8

- TMIE (Transmembrane Inner Ear Expressed Gene) – DFNB6 9
- TMC1 (Transmembrane Cochlear-Expressed Gene 1) – DFNB7 9
- TMPRSS3 (Transmembrane Serine Protease) – DFNB8/DFNB10 9
- OTOF (Otoferlin) – DFNB9 10
- CDH23 (Otocadherin) – DFNB12 10
- STRC (Stereocilin) – DFNB18 10
- USH1C (Harmonin) – DFNB18 10
- TECTA (α-tectorin) – DFNB21 11
- OTOA (Otoancorin) – DFNB23 11
- PCDH15 (Protocadherin) – DFNB23 11
- CLDN14 (Claudin 14) – DFNB29 11
- MYO3A (Myosin IIIA) – DFNB30 12
- WHRN (Whirlin) – DFNB31 12
- ESPN (Espin) – DFNB36 12
- TRIC (MARVELD) – DFNB49 13

MATERIALS and METHODS 14

- Families Studied 14
- Pedigree Analysis 14
- Blood Sampling 14
- Extraction and Purification of Genomic DNA from Blood 14
- Organic Preparation Using 1.5 ml Microcentrifuge Tubes 15
- Composition of Solutions 15

- Genomic DNA Preparation by Commercially Available Kit 16
- DNA Dilution and Micropipetting 16
- Genotyping and Primer Database Analysis 17
- Linkage to Known DFNB Loci 17
- Linkage to DFNB1 Locus (Connexin 26) 17
- Polymerase Chain Reaction (PCR) 18
- Agarose Gel Electrophoresis 18
- Polyacrylamide Gel Electrophoresis 19
- DNA Sequencing 19

RESULTS 24

- Pedigree Analysis 24
- Family 'A' 24
- Family 'B' 24
- Family 'C' 25
- Genetic Mapping of Candidate Genes for Autosomal Recessive Nonsyndromic Deafness 25

DISCUSSION 69

REFERENCES 73

Electronic Database Information 82

ACKNOWLEDGEMENTS

All praises for Almighty 'Allah' The most Merciful, without Allah's divine help, I would not have been able to achieve anything in my life. It is His benevolence and compassion that He opened new avenues and vistas of knowledge to our puny mind and choice us to serve humanity. Peace and blessings be upon the Holy Prophet Hazrat Muhammad (S.A.S), who exhorted his followers to seek knowledge from cradle to grave.

I'm feeling pride to articulate some obsession about my respected teacher and research supervisor, Dr. Wasim Ahmad, Professor and Chairman Department of Biochemistry, Quaid-i-Azam University Islamabad, without whose help this uphill task would have been impossible to achieve. I am truly inspired by him. His energy, optimism, intelligence and continuous encouragement at every step during the course of this whole project enabled me to achieve my goals. He has left an everlasting and perennial mark of his dynamic personality on my heart.

My love and affection to my parents knows no limit. I still feel like a child with his tiny finger held in his parents hands learning how to walk. My father, my ideal, I always wants to be like him, and this had led me to achieve this goal. Words become meaningless when I see them as icons of strength for being what I am today. I owe deep gratitude to my brothers and sister for their unmatched support, love and prayers. I deeply appreciate my whole family who has constantly prayed for me during my whole stay here in the university.

I also want to acknowledge the constant and diligent cooperation and support of my seniors. They profited me as per their experience and made a lot possible for me. Thanks a lot to my all lab fellows, my class fellows who not only contributed in areas of academic and research but also in sphere of friendship, sincerity and amiability.

I am thankful to my friends for their nice and sweet company and for their constructive advices. The good time spent with them can never be erased from my memories.

Zia ur Rehman

LIST OF TABLES

Table No	Title	Page No
2.1	List of microsatellite markers used for linkage to known DFNB loci.	21
2.2	Primers sequences used in screening of *GJB2* gene exon 2.	23
2.3	Sequences of primers used in screening of *TMC1* gene.	23

LIST OF FIGURES

Figure No	Title	Page No
3.1	Pedigree of family A	28
3.2	Pedigree of family B	29
3.3	Pedigree of family C	30
3.4	Electropherogram of ethidium bromide stained 8% non-denaturing polyacrylamide gel showing allele pattern obtained with marker D13S250 at 2.9 cM, linked to DFNB1 on chromosome 13q12.	31
3.5	Electropherogram of ethidium bromide stained 8% non-denaturing polyacrylamide gel showing allele pattern obtained with marker D13S292 at 8.02 cM, linked to DFNB1 on chromosome 13q12.	31
3.6	Electropherogram of ethidium bromide stained 8% non-denaturing polyacrylamide gel showing allele pattern obtained with marker D5S647 at 78.83 cM, linked to DFNB49 on chromosome 5q12.3-14.1.	32
3.7	Electropherogram of ethidium bromide stained 8% non-denaturing polyacrylamide gel showing allele pattern obtained with marker D5S2003 at 87.39 cM, linked to DFNB49 on chromosome 5q12.3-14.1.	32
3.8	Electropherogram of ethidium bromide stained 8% non-denaturing polyacrylamide gel showing allele pattern obtained with marker D11S4120 at 106.3 cM, linked to DFNB24 on chromosome 11q23.	33
3.9	Electropherogram of ethidium bromide stained 8% non-denaturing polyacrylamide gel showing allele pattern obtained with marker D11S2017 at 112.789cM, linked to DFNB24 on chromosome 11q23.	33
3.10	Electropherogram of ethidium bromide stained 8% non-denaturing polyacrylamide gel showing allele pattern obtained with marker D3S2319 at 70.93 cM, linked to DFNB6 on chromosome 3p14-21.	34
3.11	Electropherogram of ethidium bromide stained 8% non-denaturing polyacrylamide gel showing allele pattern obtained with marker D3S3582 at 74.08 cM, linked to DFNB6 on chromosome 3p14-21.	34

3.12	Electropherogram of ethidium bromide stained 8% non-denaturing polyacrylamide gel showing allele pattern obtained with marker D9S1862 at 66.55 cM, linked to DFNB7 on chromosome 9q13-21.	35
3.13	Electropherogram of ethidium bromide stained 8% non-denaturing polyacrylamide gel showing allele pattern obtained with marker D9S1806 at 68.39 cM, linked to DFNB7 on chromosome 9q13-21.	35
3.14	Electropherogram of ethidium bromide stained 8% non-denaturing polyacrylamide gel showing allele pattern obtained with marker D11S902 at 30.69 cM, linked to DFNB18 on chromosome 11p14-15.1.	36
3.15	Electropherogram of ethidium bromide stained 8% non-denaturing polyacrylamide gel showing allele pattern obtained with marker D11S23686 at 33.91 cM, linked to DFNB18 on chromosome 11p14-15.1.	36
3.16	Electropherogram of ethidium bromide stained 8% non-denaturing polyacrylamide gel showing allele pattern obtained with marker D9S302 at 123.79 cM, linked to DFNB31 on chromosome 9q32-34.	37
3.17	Electropherogram of ethidium bromide stained 8% non-denaturing polyacrylamide gel showing allele pattern obtained with marker D9S1872 at 128.65 cM, linked to DFNB31 on chromosome 9q32-34.	37
3.18	Electropherogram of ethidium bromide stained 8% non-denaturing polyacrylamide gel showing allele pattern obtained with marker D1S468 at 8.76 cM, linked to DFNB36 on chromosome 1p36.3.	38
3.19	Electropherogram of ethidium bromide stained 8% non-denaturing polyacrylamide gel showing allele pattern obtained with marker D1S214 at 19.07 cM, linked to DFNB36 on chromosome 1p36.3.	38
3.20	Electropherogram of ethidium bromide stained 8% non-denaturing polyacrylamide gel showing allele pattern obtained with marker D11S4081 at 85.51 cM, linked to DFNB2 on chromosome 11p13.5.	39
3.21	Electropherogram of ethidium bromide stained 8% non-denaturing polyacrylamide gel showing allele pattern obtained with marker D11S937 at 88.32 cM, linked to DFNB2 on chromosome 11p13.5.	39
3.22	Electropherogram of ethidium bromide stained 8% non-denaturing polyacrylamide gel showing allele pattern obtained with marker	40

D17S2196 at 50.99 cM, linked to DFNB3 on chromosome 17p11.2.

3.23 Electropherogram of ethidium bromide stained 8% non-denaturing polyacrylamide gel showing allele pattern obtained with marker D17S783 at 54.41 cM, linked to DFNB3 on chromosome 17p11.2. 40

3.24 Electropherogram of ethidium bromide stained 8% non-denaturing polyacrylamide gel showing allele pattern obtained with marker D7S501 at 117.34 cM, linked to DFNB4 on chromosome 7q31. 41

3.25 Electropherogram of ethidium bromide stained 8% non-denaturing polyacrylamide gel showing allele pattern obtained with marker D7S496 at 117.99 cM, linked to DFNB4 on chromosome 7q31 41

3.26 Electropherogram of ethidium bromide stained 8% non-denaturing polyacrylamide gel showing allele pattern obtained with marker D21S212 at 58.54 cM, linked to DFNB8 on chromosome 21q22. 42

3.27 Electropherogram of ethidium bromide stained 8% non-denaturing polyacrylamide gel showing allele pattern obtained with marker D21S1912 at 68.83 cM, linked to DFNB8 on chromosome 21q22. 42

3.28 Electropherogram of ethidium bromide stained 8% non-denaturing polyacrylamide gel showing allele pattern obtained with marker D10S1688 at 89.34 cM, linked to DFNB12 on chromosome 10q21-22. 43

3.29 Electropherogram of ethidium bromide stained 8% non-denaturing polyacrylamide gel showing allele pattern obtained with marker D10S201 at 99.44 cM, linked to DFNB12 on chromosome 10q21-22. 43

3.30 Electropherogram of ethidium bromide stained 8% non-denaturing polyacrylamide gel showing allele pattern obtained with marker D15S1044 at 38.97 cM, linked to DFNB16 on chromosome 15q21-22. 44

3.31 Electropherogram of ethidium bromide stained 8% non-denaturing polyacrylamide gel showing allele pattern obtained with marker D15S978 at 47.92 cM, linked to DFNB16 on chromosome 15q21-22. 44

3.32 Electropherogram of ethidium bromide stained 8% non-denaturing polyacrylamide gel showing allele pattern obtained with marker D11S925 at 130.7 cM, linked to DFNB21 on chromosome 11q. 45

3.33	Electropherogram of ethidium bromide stained 8% non-denaturing polyacrylamide gel showing allele pattern obtained with marker D11S4110 at 142.99 cM, linked to DFNB21 on chromosome 11q.	45
3.34	Electropherogram of ethidium bromide stained 8% non-denaturing polyacrylamide gel showing allele pattern obtained with marker D21S167 at 44.92 cM, linked to DFNB29 on chromosome 21q22.	46
3.35	Electropherogram of ethidium bromide stained 8% non-denaturing polyacrylamide gel showing allele pattern obtained with marker D21S1246 at 49.49 cM, linked to DFNB29 on chromosome 21q22.	46
3.36	Electropherogram of ethidium bromide stained 8% non-denaturing polyacrylamide gel showing allele pattern obtained with marker D13S250 at 2.9 cM, linked to DFNB1 on chromosome 13q12.	47
3.37	Electropherogram of ethidium bromide stained 8% non-denaturing polyacrylamide gel showing allele pattern obtained with marker D13S787 at 8.02 cM, linked to DFNB1 on chromosome 13q12.	47
3.38	Electropherogram of ethidium bromide stained 8% non-denaturing polyacrylamide gel showing allele pattern obtained with marker D5S2500 at 74.39 cM, linked to DFNB49 on chromosome 5q12.3-14.1.	48
3.39	Electropherogram of ethidium bromide stained 8% non-denaturing polyacrylamide gel showing allele pattern obtained with marker D5S2003 at 87.39 cM, linked to DFNB49 on chromosome 5q12.3-14.1.	48
3.40	Electropherogram of ethidium bromide stained 8% non-denaturing polyacrylamide gel showing allele pattern obtained with marker D11S4120 at 106.3 cM, linked to DFNB24 on chromosome 11q23.	49
3.41	Electropherogram of ethidium bromide stained 8% non-denaturing polyacrylamide gel showing allele pattern obtained with marker D11S2017 at 112.89 cM, linked to DFNB24 on chromosome 11q23.	49
3.42	Electropherogram of ethidium bromide stained 8% non-denaturing polyacrylamide gel showing allele pattern obtained with marker D3S3647 at 72.02 cM, linked to DFNB6 on chromosome 3p14-21.	50
3.43	Electropherogram of ethidium bromide stained 8% non-denaturing polyacrylamide gel showing allele pattern obtained with marker	50

D3S3582 at 74.08 cM, linked to DFNB6 on chromosome 3p14-21.

3.44 Electropherogram of ethidium bromide stained 8% non-denaturing polyacrylamide gel showing allele pattern obtained with marker D9S1806 at 68.39 cM, linked to DFNB7 on chromosome 9p13-21. 51

3.45 Electropherogram of ethidium bromide stained 8% non-denaturing polyacrylamide gel showing allele pattern obtained with marker D9S175 at 71.93 cM, linked to DFNB7 on chromosome 9p13-21. 51

3.46 Electropherogram of ethidium bromide stained 8% non-denaturing polyacrylamide gel showing allele pattern obtained with marker D11S902 at 30.69 cM, linked to DFNB18 on chromosome 11p14-15.1. 52

3.47 Electropherogram of ethidium bromide stained 8% non-denaturing polyacrylamide gel showing allele pattern obtained with marker D11S2368 at 33.91 cM, linked to DFNB18 on chromosome 11p14-15.1. 52

3.48 Electropherogram of ethidium bromide stained 8% non-denaturing polyacrylamide gel showing allele pattern obtained with marker D9S302 at 123.79 cM, linked to DFNB31 on chromosome 9q32-34. 53

3.49 Electropherogram of ethidium bromide stained 8% non-denaturing polyacrylamide gel showing allele pattern obtained with marker D9S1872 at 128.65 cM, linked to DFNB31 on chromosome 9q32-34. 53

3.50 Electropherogram of ethidium bromide stained 8% non-denaturing polyacrylamide gel showing allele pattern obtained with marker D1S468 at 8.76 cM, linked to DFNB36 on chromosome 1p36.3. 54

3.51 Electropherogram of ethidium bromide stained 8% non-denaturing polyacrylamide gel showing allele pattern obtained with marker D1S2660 at 14.75 cM, linked to DFNB36 on chromosome 1p36.3. 54

3.52 Electropherogram of ethidium bromide stained 8% non-denaturing polyacrylamide gel showing allele pattern obtained with marker D11S906 at 88.12 cM, linked to DFNB2 on chromosome 11p13.5. 55

3.53 Electropherogram of ethidium bromide stained 8% non-denaturing polyacrylamide gel showing allele pattern obtained with marker D11S2002 at 91.48 cM, linked to DFNB2 on chromosome 11p13.5. 55

3.54	Electropherogram of ethidium bromide stained 8% non-denaturing polyacrylamide gel showing allele pattern obtained with marker D11S2196 at 50.99 cM, linked to DFNB3 on chromosome 17p11.2.	56
3.55	Electropherogram of ethidium bromide stained 8% non-denaturing polyacrylamide gel showing allele pattern obtained with marker D11S783 at 54.41 cM, linked to DFNB3 on chromosome 17p11.2.	56
3.56	Electropherogram of ethidium bromide stained 8% non-denaturing polyacrylamide gel showing allele pattern obtained with marker D7S496 at 117.99 cM, linked to DFNB4 on chromosome 7q31.	57
3.57	Electropherogram of ethidium bromide stained 8% non-denaturing polyacrylamide gel showing allele pattern obtained with marker D7S692 at 119.61 cM, linked to DFNB4 on chromosome 7q31.	57
3.58	Electropherogram of ethidium bromide stained 8% non-denaturing polyacrylamide gel showing allele pattern obtained with marker D21S212 at 58.54 cM, linked to DFNB8 on chromosome 21q22.	58
3.59	Electropherogram of ethidium bromide stained 8% non-denaturing polyacrylamide gel showing allele pattern obtained with marker D21S1411 at 63.83 cM, linked to DFNB8 on chromosome 21q22.	58
3.60	Electropherogram of ethidium bromide stained 8% non-denaturing polyacrylamide gel showing allele pattern obtained with marker D10S1688 at 89.34 cM, linked to DFNB112 on chromosome 10q21-22.	59
3.61	Electropherogram of ethidium bromide stained 8% non-denaturing polyacrylamide gel showing allele pattern obtained with marker D10S1432 at 93.70 cM, linked to DFNB112 on chromosome 10q21-22.	59
3.62	Electropherogram of ethidium bromide stained 8% non-denaturing polyacrylamide gel showing allele pattern obtained with marker D15S1044 at 38.97 cM, linked to DFNB16 on chromosome 15q21-22	60
3.63	Electropherogram of ethidium bromide stained 8% non-denaturing polyacrylamide gel showing allele pattern obtained with marker D15S659 at 43.74 cM, linked to DFNB16 on chromosome 15q21-22.	60
3.64	Electropherogram of ethidium bromide stained 8% non-denaturing polyacrylamide gel showing allele pattern obtained with marker	61

D11S925 at 130.7 cM, linked to DFNB21 on chromosome 11q.

3.65 Electropherogram of ethidium bromide stained 8% non-denaturing polyacrylamide gel showing allele pattern obtained with marker D11S4464 at 136.99 cM, linked to DFNB21 on chromosome 11q. 61

3.66 Electropherogram of ethidium bromide stained 8% non-denaturing polyacrylamide gel showing allele pattern obtained with marker D21S1440 at 45.42 cM, linked to DFNB29 on chromosome 21q22. 62

3.67 Electropherogram of ethidium bromide stained 8% non-denaturing polyacrylamide gel showing allele pattern obtained with marker D21S1246 at 49.49 cM, linked to DFNB29 on chromosome 21q22. 62

3.68 Electropherogram of ethidium bromide stained 8% non-denaturing polyacrylamide gel showing allele pattern obtained with marker D13S633 at 2.9 cM, linked to DFNB1 on chromosome 13q12. 63

3.69 Electropherogram of ethidium bromide stained 8% non-denaturing polyacrylamide gel showing allele pattern obtained with marker D13S787 at 8.02 cM, linked to DFNB1 on chromosome 13q12. 63

3.70 Electropherogram of ethidium bromide stained 8% non-denaturing polyacrylamide gel showing allele pattern obtained with marker D5S2500 at 74.39 cM, linked to DFNB49 on chromosome 5q12.3-14.1. 64

3.71 Electropherogram of ethidium bromide stained 8% non-denaturing polyacrylamide gel showing allele pattern obtained with marker D5S2003 at 87.39 cM, linked to DFNB49 on chromosome 5q12.3-14.1 64

3.72 Electropherogram of ethidium bromide stained 8% non-denaturing polyacrylamide gel showing allele pattern obtained with marker D11S4120 at 106.3 cM, linked to DFNB24 on chromosome 11q23. 65

3.73 Electropherogram of ethidium bromide stained 8% non-denaturing polyacrylamide gel showing allele pattern obtained with marker D11S2017 at 112.89 cM, linked to DFNB24 on chromosome 11q23. 65

3.74 Electropherogram of ethidium bromide stained 8% non-denaturing polyacrylamide gel showing allele pattern obtained with marker D3S3647 at 70.02 cM, linked to DFNB6 on chromosome 3p14-21. 66

3.75	Electropherogram of ethidium bromide stained 8% non-denaturing polyacrylamide gel showing allele pattern obtained with marker D3S3582 at 74.08 cM, linked to DFNB6 on chromosome 3p14-21.	66
3.76	Electropherogram of ethidium bromide stained 8% non-denaturing polyacrylamide gel for marker D9S301 at 68.13 cM on chromosome 9p13-21.	67
3.77	Electropherogram of ethidium bromide stained 8% non-denaturing polyacrylamide gel for marker D9S1806 at 68.39 cM on chromosome 9p13-21.	67
3.78	Electropherogram of ethidium bromide stained 8% non-denaturing polyacrylamide gel for marker D9S1876 at 69.4 cM on chromosome 9p13-21.	68
3.79	Electropherogram of ethidium bromide stained 8% non-denaturing polyacrylamide gel for marker D9S175 at 71.93 cM on chromosome 9p13-21.	68

LIST OF ABBREVIATIONS

AP	Ammonium persulphate
ARSNHL	Autosomal recessive non-syndromic hearing loss
ATP	Adenine triphosphate
bp	Base pairs
CDH23	Cadherins23
CD36	Leukocyte differentiation antigen CD36
cDNA	Complimentary DNA
CHLC	Cooperative human linkage center
CLDN	Claudin
cM	CentiMorgan
CMV	Cyotmegalovirus
COCH	Cochlin
COL	Collagen
Cx	Connexin
dB	Decibels
DFN	Deafness
DFNA	Autosomal dominant non-syndromic deafness
DFNB	Autosomal recessive non-syndromic deafness
dNTPs	Deoxyribo nucleotide triphosphates
DNA	Deoxyribonucleic acid
DNR	Dinucleotide repeats
EDTA	Ethylene diamine tetra acetic acid
ESPN	Espin
ESTs	Expressed sequence tags
EVA	Enlarge vestibular aqueduct
GJB	Gap junction protein
HGF	Hepatocyte growth factor
HI	Hearing impairment
DCNQ4	Potassium voltage-gate channel, KQT-like subfamily, member 4

kDa	kiloDaltons
$MgCl_2$	Magnesium chloride
mM	Milli Molar
mRNA	Messenger RNA
mtRNA	Mitochondrial RNA
MTRNR1	Mitochondrially encoded 12S RNA
MYH	Myosin, heavy polypeptide
MYO	Myosin
NaCl	Sodium chloride
NF	Neurofibromatosis
ng	Nanogram
NSHI	Non-syndromic hearing impairment
NSRD	Non-syndromic recessive deafness
OD	Optical density
OMIM	Online Mendelian inheritance in man
OSMED	Otospondylomegaepiphyseal dysplasia
OTOA	Otoancorin
OTOF	Otoferlin
PCDH	Protocadherin
PCR	Polymerase chain reaction
PDS	Pendred syndrome
POU4F3	POU domain, class 4, transcription factor 3
RNA	Ribonucleic acid
RT-PCR	Reverse transcriptase-polymerase chain reaction
SDS	Sodium dodecyl sulphate
sh-1	Shaker-1
SLC26A4	Solute carrier family 26, member 4
SNHL	Sensorineural hearing loss
STRC	Stereocilin
TBE	Tri-borate EDTA
TECTA	Tectorin

TEMED	N'N'N'N-tetra methyl ethylene diamine
TetraNR	Tetranucleotide repeat
Tg	Thyroglobin
TMC1	Transmembrane channel like gene 1
TMIE	Transmembrane inner ear
TMPRSS3	Transmembrane serine protease
TriNR	Trinucleotide repeat
TRIC	Tricellulin
T.S.R	Template suppression reagent
µl	Microlitre
USH	Usher syndrome
UV	Ultra violet
WFS1	Wolfram syndrome 1
WHRN	Whirlin

ABSTRACT

Hearing loss is complete or partial decrease in the ability to detect or understand sound. The incidence of congenital hearing loss is estimated at 1 in 1000 births, of which approximately equal numbers of cases are attributed to environmental and genetic factors. After 1995, when first gene for hearing loss was identified, a great number of new genes have been characterized to date for hearing loss. Of the hearing loss disorders attributable to genetic causes, ~70% are classified as non-syndromic and the remaining 30% are syndromic deafness. Non-syndromic hearing impairment can be further subdivided by mode of inheritance: ~77% of cases are autosomal recessive, 22% are autosomal dominant, 1% are X-linked and < 1% are due to mitochondrial inheritance.

In the study, presented here, three Pakistani families A, B and C demonstrating autosomal recessive form of non-syndromic deafness were analyzed. Linkage in all the three families were searched by using polymorphic microsatellite markers corresponding to candidate genes involved in autosomal recessive non-syndromic deafness phenotypes. In the family 'A' with four affected and family 'B' with six affected individuals, several known DFNB loci including DFNB1 locus harboring *GJB2* gene were excluded from linkage. The family 'C' with two affected individuals showed linkage to DFNB7/11 on chromosome 9q13-21. Sequence analysis of all the 24 exons and splice junctions of *TMC1* gene, located at DFNB7/11 locus, failed to identify any functional sequence variant. Therefore, it is possible that the mutation is located in the regulatory sequences of the *TMC1* gene.

Introduction

INTRODUCION

Hearing impairment is a full or partial decrease in the ability to detect or understand sounds and is caused by a wide range of biological and environmental factors. Loss of hearing can happen to any organism that perceives sound. It is a major public health concern because it affects 6-8% of the population in developed nations when all causes are combined and it is the most common birth defect (Petit *et al.*, 2001). The incidence of congenital hearing loss is estimated at 1 in 1000 births, of which approximately equal numbers of cases are attributed to environmental and genetic factors (Morton, 1991; Gorlin *et al.*, 1995).

Environmental factors leading to hearing loss include acoustic trauma, ototoxic drugs (e.g., aminoglycosides), and bacterial and viral infections. Of the hearing-loss disorders attributable to genetic caused, ~70% are classified as non-syndromic, in which there are no additional abnormalities, and the remaining 30% are syndromic deafness, in which deafness is accompanied by other specific abnormalities. Hundreds of syndromic forms of deafness have been described, and the underlying genetic mutation has been identified for many of the more common forms (Gorlin *et al.*, 1995; Steel and Kros, 2001). Among the many disorders classified as syndromic hearing loss, the pathology varies widely, but in non-syndromic deafness, the defect is generally senorineural.

Non-syndromic hearing impairment can be further subdivided by mode of inheritance: ~77% of cases are autosomal recessive, 22% are autosomal dominant, 1% are X-linked, and <1% are due to mitochondrial inheritance (Morton, 1991). Dominant loci are denoted with the prefix "DFNA," recessive loci with "DFNB," X-linked loci with "DFN," and modifying loci with "DFNM." They are numbered in chronological order of discovery. Between 1997 and today, many non-syndromic hereditary forms of deafness have been localized on the human genome by genetic linkage techniques.

Generally, patients with autosomal recessive hearing impairment have prelingual and profound deafness, and patients with autosomal dominant hearing impairment have progressive and postlingual hearing impairment. This observation may be explained by the complete absence of functional protein in patients with recessive disorders, whereas, in patients with autosomal dominant disorders, dominant mutations may be

consistent with initial function and subsequent hearing impairment due to accumulation of pathology (Resendes *et al.*, 2001).

Mechanism of Hearing

Sound is a form of energy that moves through air, water, and other matter, in waves of pressure. Sound is the means of auditory communication, including frog calls, bird songs, and spoken language. Although the ear is the vertebrate sense organ that recognizes sound, it is the brain and central nervous system that "hears". Sound waves are perceived by the brain through the firing of nerve cells in the auditory portion of the central nervous system. The ear changes sound pressure waves from the outside world into a signal of nerve impulses sent to the brain.

Human can generally hear sounds with frequency between 20 Hz and 20 kHz. Human hearing is able to discriminate small difference in loudness (intensity) and pitch (frequency) over that large range of audible sound. This healthy human range of frequency detection varies significantly with age, occupational hearing damage, and gender, some individual are able to hear pitches up to 22 kHz and perhaps beyond, while some other are limited to about 16 kHz. The ability of most adults to hear sounds above about 8 kHz begins to deteriorate in early middle age.

The process of transduction whereby sound impulses reaching the inner ear are converted into neural impulses to the brain is enormously complex (Parkinson and Brown, 2002). The mammalian ear responds to sounds with a speed, sensitivity and a frequency resolution that make it the doyen of signaling systems (Hudspeth, 1997).

Hearing begins when sound waves that travel through the air reach the outer ear or pinna, which is the part of ear that we can see. In humans, amplification of sound ranges from 5 to 20 dB for frequencies within the speech range (about 1.5 - 7 kHz). Since the shape and length of the human external ear preferentially amplifies sound in the speech frequencies, the external ear also improves signal to noise ratio for speech sounds (John and Matthew, 2002).

The sound waves then travel from the pinna through the ear canal to the middle ear, which includes the tympanic membrane or eardrum (a thin layer of tissue) and three bones called ossicles. When the eardrum vibrates, the ossicles amplify these vibrations and carry them to the inner ear.

The inner ear is made up of a snail-shaped chamber called the cochlea, which is filled with fluid and lined with thousands of tiny hair cells (outer and inner rows). Our sense of hearing originates from 16,000 hair cells in each cochlea (Wright *et al.*, 1987). When the vibrations move through this fluid, the tiny hair cells translate them into electrical nerve impulses and send them to the auditory nerve, which connects the inner ear to the brain. When these nerve impulses reach the brain, they are interpreted as sound. The cochlea is like a piano so that specific areas along the length of the cochlea pick up gradually higher pitches.

Types of Hearing Loss

All forms of deafness can be broadly classified as conductive, perceptive and mixed type.

- **Conductive hearing loss** results from a problem with the outer or middle ear, including the ear canal, eardrum, or ossicles.
- **Perceptive or sensorineural hearing loss** results from damage to the inner ear (cochlea), auditory nerve, or the auditory region of the brain (Beighton, 1983). The most common type is caused by the outer hair cells not functioning correctly.
- **Mixed hearing loss** occur when someone has both conductive and sensorineural hearing problems.

Degree of Hearing Loss

Results of the audiometric evaluation are plotted on a chart called an audiogram. Hearing loss is measured in decibels (dB) and is described in general categories. The American National Standards Institute (1969) has categorized hearing loss in terms of decibels into following categories.

- Slight 16-25 dB loss
- Mild:
    - for adult: 25-40 dB loss
    - for children: 15-40 dB loss
- Moderate 41-55 dB loss

- Moderately severe 56-70 dB loss
- Severe 71-90 dB loss
- Profound 90 dB loss or more

Causes of Hearing loss

Causes of hearing loss can be broadly categorized into two categories. An acquired or environmental cause and genetic or heritable cause. Acquired deafness associated with age or noise exposure is more common than genetic deafness by roughly 2 orders of magnitude, congenital deafness occurs in 1 per every 1000-2000 births with autosomal recessive inheritance being the most common form. All types of early-onset hereditary deafness currently observed are due to monogenic defects (Petit *et al.*, 2001; Freidman and Griffith, 2003) with the exception of few cases in which digenic inheritance has been suggested. Non-inherited abnormalities of the inner ear such as the Mondini malformation, account for roughly 20% of congenital sensorineural deafness. The bulk of the remaining, genetic deafness is non-syndromic, meaning that it does not have any obvious distinguishing features.

Environmental Causes

It is commonly results from prenatal infections from "TORCH" organisms (i.e., toxoplasmosis, rubella, cytomegalic virus, and herpes), or postnatal infections, particularly bacterial meningitis caused by Neisseria meningitides, Haemophilus influenza, or Streptococcus pneumoniae. Meningitis from many other organisms, including Escherichia coli, Listeria monocytogenes, Streptococcus agalactiae, and Enterobacter cloacae, can also cause hearing loss. Asymptomatic congenital cytomegalovirus (CMV) infection is often unrecognized and can be associated with variable, fluctuating, sensorineural hearing loss (Harris *et al.*, 1984; Hicks *et al.*, 1993). Similarly prematurity, exposure to ototoxic medications and trauma can also cause acquired hearing loss in children (Schrijver, 2004).

Genetic or Heritable causes

Genetic hearing loss has diverse etiologies and it is estimatd that approximately 1% of all human genes are involved in the hearing process (Friedman and Griffith, 2003). About 1 child in 1000 is born with prelingual hearing loss, of which about half have genetically determined hearing loss (Morton, 1991; Davis and Parving, 1994).

Genetic hearing loss may be either due to mutation in single gene (monogenic forms) or from a combination of mutations in different genes and environmental factors (multifactorial forms).

Genetic scientists subdivide causes of genetic hearing loss into two general categories: "Non-Syndromic" and "Syndromic". Syndromic hearing loss is associated with malformations of the external ear or other organs or with medical problems involving other organ systems. Non-syndromic hearing loss on the other hand has no associated visible abnormalities of the external ear, nor is there any related medical problems; however, it can be associated with abnormalities of the middle ear and/or inner ear. By far, the more common is Non-syndromic hearing loss which includes 2/3 of all genetic hearing losses.

Syndromic Hearing impairment

Over 400 genetic syndromes that include hearing loss have been described (Gorlin *et al.*, 1995). Syndromic hearing impairment may account for up to 30% of prelingual deafness, but its relative contribution to all deafness is much smaller, reflecting the occurrence and diagnosis of post lingual hearing loss.

In syndromic cases of deafness the affected individuals have a specific pattern of additional clinical features, which are not related to audition. It may accounts for 30% of all genetically determined cases. Syndromic deafness can be either dominant (Wardenburg syndrome, Branchial-oto-renal syndrome, Stickler syndrome), recessive (Ushers syndrome, Pendred syndrome), X-linked (Alport syndrome, Nance syndrome, Hunter syndrome) or mitochondrial.

Non-syndromic Hearing loss

More than 70% of hereditary hearing loss is non-syndromic (Cremers *et al.*, 1991; Van Camp *et al.*, 1997). Non-syndromic hearing loss is extraordinarily heterogeneous and approximately 100 localizations have been reported across the genome as sites of genes causally related to non-syndromic hearing impairment, and 37 different genes encoding proteins with a wide variety of functions have been identified. In the field of non-syndromic hearing loss 21 genes associated with autosomal recessive inheritance, 20 associated with autosomal dominant inheritance, and one with X-linked recessive transmission have been identified and characterized.

Genes Implicated in Hearing Loss

GJB2 (Connexin 26)

Mutations in the connexin 26 (Cx26) gene (*GJB2*), which is located on chromosome 13q11-12, are associated with the autosomal recessive non-syndromic neurosensory deafness known as "DFNB1" (Chaib *et al.*, 1994; Kelsell *et al.*, 1997; Van Camp *et al.*, 1997; Zelante *et al.*, 1997). These studies indicated that DFNB1 cause 20% of all childhood deafness and may have a carrier rate as high as 2.8%.

The *GJB2* gene has a single coding exon and the protein belongs to the large family of connexins having four transmembrane domains, which have been implicated in gap-junctional intercellular communication (Kumar and Gilula, 1996). Six connexin subunits bind together to form a hexamer (connexon) in plasma membrane, and each connexin associates with another connexin in an adjacent cell to form an intercellular channel; and multiple channels, in turn, cluster in a specialized membrane region to form a gap junction.

Connexons are important for recycling of potassium ions into the cochlear endolymph through the network of gap junctions that extends from the epithelial supporting cells to the fibrocytes of the spiral ligament and to the epithelial marginal cell of the stria vascularis. The ion homeostasis is essential for normal hearing, and mutations in several genes encoding connexins or ion channels lead to hereditary deafness (Holt and Corey, 1999; Steel, 1999; Rabionet *et al.*, 2000).

Mutations in the *GJB2* gene represent a major cause of pre-lingual, non-syndromic, recessive deafness, as they are responsible for as much as 50% of such cases in many populations. One specific mutation, the 35delG mutation, accounts for the majority of the *GJB2* mutations detected in Caucasian populations and represents one of the most frequent disease mutations identified so far (Denoyelle *et al.*, 1997; Estivill *et al.*, 1998). The 35delG mutation consists of a deletion of a guanine (G) in a sequence of six Gs extending from position 30–35 leading to a frameshift and premature stop codon at nucleotide 38 (Zelante *et al.*, 1997; Denovelle *et al.*, 1997).

Mutations in the *GJB2* gene are also responsible for syndromic forms of hearing loss, including autosomal-dominant mutilating keratoderma with sensorineural deafness (Vohwinkel syndrome), other forms of autosomal-dominant palmoplantar keratoderma with deafness, and the ectodermal dysplasia keratitis–ichtyosis–deafness

syndrome. Most of these *GJB2* mutations are located in the first extracellular domain (Guilford *et al.*, 1994; Kelsell *et al.*, 1997).

***GJB6* (Connexin 30)**

A role for *GJB6*, the gene adjacent to *GJB2* on chromosome 13, was first suggested in 1999, when a dominant mutation (T5M) was described (Grifa *et al.*, 1999). The most common mutation in *GJB6*, however, is a 300-kb deletion which causes non-syndromic SNHL when homozygous, or when present on the opposite allele of a *GJB2* mutation. *GJB2* and *GJB6* are only 35 kb apart. *GJB2* is located on the centromeric side. *GJB6* is very similar to *GJB2*, but not interrupted by introns (Grifa *et al.*, 1999). Both genes are expressed in the cochlea where they can combine to form multi-unit hemichannels in the cell membrane, and function as an integral component of the potassium regulation in the inner ear.

GJB6 has also been associated with Clouston syndrome (hydrotic ectodermal dysplasia), which is autosomal dominant and may occur with deafness (Lamartine *et al.*, 2000; Smith *et al.*, 2002).

***GJB3* (Connexin 31)**

The *GJB3* gene encoding the gap junction protein connexin 31 was cloned and mapped to chromosome 1p35-p33. Currently, non of the known DFNB loci maps to the 1p35-p33 chromosomal region.

The predicted *GJB3* protein connexin 31 has four hydrophobic transmembrane domain-like motifs, a structure similar to that of the other connexins and sharing 76% homology with human *GJB2*.

***MYO7A* (Myosin VIIA) - DFNB2**

Myosin genes are members of a large superfamily of genes that encode proteins that exert mechanical forces. The myosins are molecular motors that bind to actin filaments and move along them. They have many functions, including transport of intracellular organelles, phagocytosis, secretion, muscular contraction, and cellular movement (Cheney *et al.*, 1993; Mooseker and Cheney, 1995). Myosins in the ear may use actin filaments as tracks to transport intracellular vesicles in the hair cells. Myosins are present in stereocilia, which are filled with actin, and in the cuticular plate, which is actin-rich. Therefore, they might provide an anchor for actin in the hair

cells and their stereocilia and be responsible not only for the tension on the tip links of the stereocilia and their movements, but also for the overall cytoskeletal organization of hair cells.

The *MYO7A* gene is a typical unconventional myosin consisting of 48 coding exons (Weil *et al.*, 1997). Expression was found in several mouse and human tissues, including the retina and cochlea (Weil *et al.*, 1995; Weil *et al.*, 1996).

More than 50 distinct *MYO7A* mutations have been reported in USH1B, four different mutations have been found in DFNB2, and two in dominant deafness (DFNA11). The mutations are dispersed throughout the *MYO7A* gene (Janecke *et al.*, 1999).

***MYO15* (Myosin XV) – DFNB3**

Full-length human myosin XV is encoded by 66 exons, and expression studies demonstrated that *MYO15* is expressed in a number of tissues in addition to the inner ear (Wang *et al.*, 1998). In the shaker-2 mouse, the presence of very short stereocilia, and a long abnormal actin-containing structure that projects from the base of auditory hair cells, suggested that myosin XV is necessary for actin organization in hair cells (Probst *et al.*, 1998; Anderson *et al.*, 2000).

***SLC26A4* (Pendrin) – DFNB4**

The *SLC26A4* encodes a transmembrane protein pendrin, which functions as a transporter of chloride and iodide and is expressed in the thyroid gland, the inner ear, and the kidney. Functional studies showed that mutations associated with Pendred syndrome have complete loss of chloride and iodide transport, while mutant alleles in patients with DFNB4 are able to transport both iodide and chloride, although at a much lower level than wild-type pendrin (Scott *et al.*, 2000). To explain the associated temporal bone abnormalities, it has been hypothesized that *SLC26A4* controls fluid homeostasis in the membranous labyrinth, which in turn affects development of the bony labyrinth (Campbell *et al.*, 2001).

Enlarged vestibular aqueduct (EVA) is a frequent symptom in patients with Pendred syndrome state, but it can also be present as an isolated finding together with sensorineural hearing loss. In the majority of cases, one or two *SLC26A4* mutations have been identified.

TMIE (Transmembrane Inner Ear Expressed Gene) – DFNB6

On the basis of conserved synteny between distal mouse chromosome 9 and human chromosome 3p, the spinner strain of deaf mice was suggested to be the mouse model for human DFNB6 hearing loss (Fukushima *et al.*, 1995). Mutations in the novel gene *Tmie* were found to be responsible for hearing loss and vestibular dysfunction in spinner mice, and subsequently homozygous mutations in the human ortholog *TMIE* were detected in the five DFNB6 families (Fukushima *et al.*, 1995; Naz *et al.*, 2002).

The predicted *TMIE* protein exhibited no significant similarity to any known protein, and expression was demonstrated in many human tissues (Naz *et al.*, 2002).

TMC1 (Transmembrane Cochlear-Expressed Gene 1) – DFNB7

The *TMC1* gene was shown to belong to a family of transmembrane channel-like (TMC) genes with eight paralogs (*TMC1–TMC8*) predicted to encode proteins with 6–10 transmembrane domains and a novel conserved 120-amino acid sequence termed the *TMC* domain (Kurima *at al.*, 2002).

The mutations identified in *TMC1* gene include nonsense, frameshift, missense, genomic deletion, and splice-site mutations, all in homozygous state (Santos *et al.*, 2005).

TMPRSS3 (Transmembrane Serine Protease) – DFNB8/DFNB10

The *TMPRSS3* gene has 13 exons encoding transmembrane (TM), low-density-lipoprotein receptor A (LDLRA), scavenger-receptor cysteine-rich (SRCR), and serine protease domains similar to other proteases (Scott *et al.*, 2001).

The mouse ortholog of *TMPRSS3* is expressed in the spiral ganglion, the cells supporting the organ of Corti and the stria vascularis, primarily in the endoplasmic reticulum membranes (Guipponi *et al.*, 2002). The epithelial sodium channel EnaC, which is involved in the regulation of sodium concentration in the endolymph, was found to have a similar expression as Tmprss3 in rat inner ear. Consequently, it was suggested that EnaC was a substrate for *TMPRSS3*. Functional expression studies in Xenopus laevis oocytes demonstrated that *TMPRSS3* significantly activates ENaC, whereas *TMPRSS3* missense mutations causing DFNB8/DFNB10 deafness failed to activate ENaC in this model (Guipponi *et al.*, 2002).

OTOF (Otoferlin) – DFNB9

OTOF mutations have been described in non-syndromic, recessive auditory neuropathy, which is characterized by moderate to profound, sensorineural hearing loss with normal otoacoustic emissions (OAEs), indicating preserved outer hair cell function, and lack of any other detectable peripheral neuropathy and with no benefit from hearing aids (Varga *et al.*,2003; Tekin *et al.*, 2005).

The human *OTOF* gene was shown to be composed of 48 coding exons predicting a 1997 amino acid protein otoferlin with alternatively spliced transcripts predicting several long isoforms (with six C2 domains) and short isoforms (three C2 domains) (Yasunaga *et al.*, 2000).

CDH23 (Otocadherin) – DFNB12

The *CDH23* gene belongs to the cadherin superfamily of intercellular adhesion proteins that typically have large extracellular domains (characterized by cadherin repeats that have been demonstrated to provide cell-to-cell adhesion), a membrane-spanning region, and cytoplasmic domains highly divergent among family members.

Recent mouse data have implicated cadherin 23, harmonin and myosin VIIa in a single functional network essential to ensure the cohesion of the stereocilia of the hair bundle. *CDH23* was recently shown to be part of the tip links involved in cross-linking stereocilia (Di Palma *et al.*, 2001; Siemens *et al.*, 2004).

STRC (Stereocilin) – DFNB18

The *STRC* gene contains 29 coding exons and was shown to be tandemly duplicated with a stop codon in exon 20 in the B copy, which might represent a pseudogene. The deduced protein stereocilin shows no significant homology to any other known protein (Verpy *et al.*, 2001). Immunofluorescence studies demonstrated that in the mouse inner ear, stereocilin is expressed only in the sensory hair cells, with intense staining along the hair bundle composed of stereocilia (Verpy *et al.*, 2001).

USH1C (Harmonin) – DFNB18

The *USH1C* gene was shown to contain 28 exons and encodes a PDZ domain-containing protein, harmonin (from the Greek word armonia, meaning 'assembling in a correct order). Immunohistofluorescence detected harmonin in the sensory areas of

the inner ear, especially in the cytoplasm and stereocilia of hair cells (Verpy *et al.*, 2000)

Eight different transcripts were identified in mouse inner ear. Harmonin was shown to bind to otocadherin and to interact with myosin VIIA suggesting a functional unit underlying the formation of a coherent hair cell bundle (Siemens *et al.*, 2002).

***TECTA* (α-tectorin) – DFNB21**

TECTA encodes a-tectorin, one of the major non-collagenous extracellular matrix components of the tectorial membrane that bridges the stereocilia bundles of the sensory hair cells. Mice homozygous for a targeted deletion in a-tectorin have tectorial membranes that are detached from the cochlear epithelium and lack all non-collagenous matrix (Legan *et al.*, 2000).

***OTOA* (Otoancorin) – DFNB23**

Otoancorin was suggested to mediate attachment of the tectorial membrane in the cochlea, and the otoconial membranes and cupulae in the vestibule. The corresponding human gene, *OTOA*, consists of 28 exons and maps to chromosome 16p12.2 (Zwaenepoel *et al.*, 2001). *OTOA* mutations are not frequent causes of deafness and occur very rarely.

***PCDH15* (Protocadherin) – DFNB23**

The *PCDH15* gene encoding protocadherin 15 had been shown to be responsible for Usher syndrome type 1F (Ahmad *et al.*, 2001), whereas recessive mutations of *Pcdh15* cause deafness in the Ames waltzer (av) mouse (Alagramam *et al.*, 2001). The *PCDH15* gene was therefore thought to be a good candidate for non-syndromic hereditary deafness.

Protocadherin 15 immunoreactivity has been detected in mouse retinal photoreceptors, organ of Corti and vestibular hair cells. The immunoreactivity was seen along the length of stereocilia, in the cuticular plate, and diffusely distributed in the cytoplasm of inner and outer hair cells (Ahmad *et al.*, 2003).

***CLDN14* (Claudin 14) – DFNB29**

Claudins comprise a multigene family of integral membrane proteins identified as major cell adhesion molecules working at intercellular tight junctions (Tsukita *et al.*, 2000). Immunofluorescence studies in the mouse at postnatal day 4 demonstrated

claudin 14 expression in the inner and outer hair cell region of the organ of Corti and in the sensory epithelium of the vestibular organs.

It has been hypothesized that the absence of claudin 14 from tight junctions in the organ of Corti leads to altered ionic permeability of the paracellular barrier of the reticular lamina and that prolonged exposure of the basolateral membranes of outer hair cells to high potassium concentrations may be the cause of cell death of hair cells (Ben-Yosef *et al.*, 2003).

***MYO3A* (Myosin IIIA) – DFNB30**

Myosin IIIA is an actin-dependent motor protein belonging to the class III unconventional myosins with 36% identity to Drosophila *NINAC*, mutations of which cause retinal degeneration (Doze and Burnside, 2000).

As the motor domain of the *MYO3A* peptide most closely resembles human myosin VIIA, it is probable that *MYO3A* has a function in the mechanotransduction process, but the exact function in the mammalian ear remains to be investigated. Myosin IIIA expression had previously been demonstrated in human retina (Doze and Burnside, 2000), and murine expression was shown in cochlea, where it was restricted to the neurosensory epithelium, especially to inner and outer hair cells (Walsh *et al.*, 2002).

***WHRN* (Whirlin) – DFNB31**

The human gene was shown to comprise 12 exons with three PDZ domains and one proline-rich domain, the closest related protein being harmonin, which also contains three PDZ domains (Mburu *et al.*, 2003).

Immunofluorescence studies in the mouse showed whirlin expression overlapping with actin staining in stereocilia at the growing ends of actin filaments (Mburu *et al.*, 2003). The findings suggest that whirlin acts by controlling actin polymerization and membrane growth of stereocilia (Mburu *et al.*, 2003; Kikkawa *et al.*, 2005).

***ESPN* (Espin) – DFNB36**

The human *ESPN* gene consists of 13 exons and was predicted to encode an 854 amino acid protein with eight ankyrin repeats, two proline-rich regions, an actin-binding WH2 domain, and a coiled coil domain important for actin bundling (Naz *et al.*, 2004). The espins are actin-bundling proteins. In both the cochlea and vestibule of the mouse inner ear, espin was localized mostly to the stereocilia (Zheng *et al.*, 2000).

Espin was absent from the stereocilia of jerker mice, eventually leading to complete loss of all sensory hair cells (Zheng *et al.*, 2000).

TRIC (*MARVELD*) – **DFNB49**

Tricellulin was recently described as one of the constituents of tricellular Tight Junctions (tTJs) and perhaps of bicellular Tight Junctions (bTJs) of epithelial barriers in general.

Mutant alleles of *TRIC*, which encodes tricellulin, co-segregate with non-syndromic moderate-to-profound DFNB49. In the inner ear, tricellulin is concentrated at the tricellular TJs in cochlear and vestibular epithelia, including the structurally complex and extensive junctions between supporting and hair cells. Multiple alternatively spliced isoforms of *TRIC* in various tissues and mutations of *TRIC* associated with hearing loss remove all or most of a conserved region in the cytosolic domain that binds to the cytosolic scaffolding protein ZO-1. In human, the longest *TRIC* mRNA (*TRIC-α*) has seven exons, which are predicted to encode four transmembrane domains and an occluding-ELL domain located at the C-terminus.

TRIC-α is predicted to encode a protein of 558 amino acids, whereas the *TRIC-α1* massage lacks exon 3 the C-terminus of the *TRIC-α* and in *TRIC-α1* isoforms, there is a 103-aa residue occludin-ELL domain that is 32% identical (51% similar) to a region of the C-terminus of occludin. In contrast, *TRIC-b* is a shorter isoform which encodes 458 amino acids protein lacking the occludin-ELL domain. *TRIC-c*, which encodes 442 amino acids, was cloned from mRNA isolated from human lung.

A possible reason for the deafness phenotype due to mutations of *TRIC* is that the reticular lamia in the organ of Corti is less rigid, leading either to abnormalities in stereocilia microdeflections or to the inability of the reticular lamina to withstand the mechanical stress of outer hair-cell motility (Ramzan *et al.*, 2005; Riazuddin *et al.*, 2006).

In the present study three families with non-syndromic autosomal recessive deafness have been investigated. Genetic mapping was performed by genotyping with microsatellite markers. In addition, *TMC1* gene was sequenced in a family linked to DFNB7/11 on chromosome 9.

Materials and Methods

MATERIALS and METHODS

Families Studied

For the study presented here, three consanguineous families referred herewith as A, B and C with autosomal recessive nonsyndromic hearing impairment were ascertained from different regions of Pakistan. The families were visited at their places of residence to generate pedigrees and collect other relevant information. Informed consent was obtained from the parents of the affected children and all other family members who participated in the study. The information obtained was crosschecked by interviewing different family members. Blood samples from affected and normal individuals of each family were collected for DNA extraction.

Pedigree Analysis

For genetic implication an extensive pedigree was constructed for each family by the standard methods described by Bennett *et al.* (1995). The pattern of inheritance of the disease was deduced by observing the mode of segregation or transmission within family. The exact genealogical relationships for all the affected individuals were obtained through extensive personal interviews of elders of the families. Males were symbolized by squares and females by circles. The normal individuals were designated with unfilled symbols while the affected individuals by filled symbols. Each generation was indicated by Roman numeral. The individuals within a generation were designated by Arabic numerals. Double lines in the pedigrees represent the consanguineous marriages. A number enclosed within a symbol indicates the number of sibs.

Blood Sampling

Blood samples from both affected and normal members of the family were collected using 10 ml syringes (0.7 X 40 mm, 22 G X $1^{1/2}$) and from children (below 2 years of age) by butterflies, in standard potassium EDTA vacutainer tubes. The blood samples collected were stored at 4°C.

Extraction and Purification of Genomic DNA from Blood

Two methods were used for the extraction and purification of the Human Genomic DNA from blood samples:

- Organic preparation using 1.5 ml microcentrifuge tubes
- Commercially available kit

Organic Preparation Using 1.5 ml Microcentrifuge Tubes

Genomic DNA was prepared by using phenol/Chloroform method. Approximately 0.75 ml of blood was taken in a 1.5 ml microcentrifuge tube along with 0.75 ml solution A and was kept at room temperature for 5-10 minutes after mixing the contents. The tube was then centrifuged for 1 minute at 13,000 rpm in a Microfuge® 18 centrifuge (Beckman Coulter™ USA). Supernatant was discarded and pellet was resuspended in 400 µl of solution A. Centrifugation was repeated and after discarding the supernatant the nuclear pellet was resuspended in 400 µl of solution B, 12 µl of 20% SDS and 5 µl of proteinase K and incubated at 37°C over night. On the following day 0.5 ml of a fresh mixture of equal volume of solution C and solution D was added in sample, mixed and centrifuged for 10 minutes at 13,000 rpm. The aqueous phase (upper layer) was collected in a new tube and equal quantity of solution D was added. Centrifugation was then carried out again at 13,000 rpm for 10 minutes. The aqueous phase was placed in a new tube and after adding 55 µl of 3 M sodium acetate (pH 6) and equal volume of isopropanol. Tubes were then inverted several times to precipitate DNA. The DNA pellet was washed with 70% ethanol and dried in the concentrator for 8-10 minutes at 45°C. After evaporation of residual ethanol, DNA was dissolved in appropriate amount (150-200 µl) of DNA dissolving buffer (Tris-EDTA i.e. TE).

Composition of Solutions

Solution A

0.32 M Sucrose

10 mM Tris (pH 7.5)

5 mM $MgCl_2$

1 % (v/v) Triton X-100

Solution B

10 mM Tris (pH 7.5)

400 mM NaCl

1 mM EDTA (pH 8.0)

Solution C

Phenol

10 mM Tris

Solution D

Chloroform 24 volumes

Isoamyl alcohol 1 volume

DNA Dissolving Buffer

10 mM Tris (pH 8.0)

0.1 mM EDTA

Genomic DNA Preparation by Commercially Available Kit

DNA extraction was also carried out using Genomic DNA Isolation Kit (Sigma Chemical Co. USA). One hundred and fifty microlitre of blood was taken in a 1.5 ml microcentrifuge tube along with 250 µl of lysis solution A; mixed by inversion, incubate at 65°C for 6 minutes. Clear aqueous phase was transferred to a new 1.5 ml microcentrifuge tube after adding 100 µl of precipitation solution B and centrifugation at 14,000 rpm for 5-10 minutes. DNA was then precipitated by adding 500 µl of 100% ethanol. Ethanol was removed after centrifugation at maximum speed for 2 minutes, and then washed with 70% ethanol. After evaporation of residual ethanol DNA was dissolved in appropriate amount of Tris-EDTA (TE) buffer by incubation at 65°C for 5 minutes.

DNA Dilution and Micropipetting

Genomic DNA was quantified by taking optical density (OD) at 260 nm wavelength and subsequently diluted to 40-50 ng/µl for PCR amplification by using GeneRay UV-Photometer (Biometra® , Germany). Micropipetting was carried out by using adjustable micropipettes with autoclaved disposable tips, ranging from 10-1000 µl of upper volume limit.

Genotyping and Primer Database Analysis

In the present study several candidate loci was tested by typing microsatellite markers linked to loci. The number of tri- and tetra-nucleotides repeat sequence polymorphic markers used in present study was approximately 94%. Average heterozygosity of each marker was above 70%, implying that these markers are highly informative for allelotyping pedigree members. The autosomal recessive non-syndromic hearing impairment loci initially investigated and the microsatellite markers with their cytogenetic location are shown in the Table 2.1.

Microsatellite markers mapped by Cooperative Human Linkage Centre (CHLC), were obtained from Research Genetics, Inc. (USA). The cytogenetic locations of these markers, their heterozygosity as well as the length of the amplified products were obtained from genome database homepage (www.gdb.org) and Marshfield Medical Center (www.marshmed.org/genetics/).

Linkage to Known DFNB Loci

To elucidate the gene defect in the family 'A' 'B' and 'C', an initial search for linkage was carried out by using polymorphic markers mapped within several autosomal recessive non-syndromic deafness loci listed on the Hereditary Hearing Loss Homepage (http://dnalab-www.uia.ac.be/dnalab/hhh).

Table 2.1 summarizes microsatellite markers located in the region of known deafness loci, which were used as first pass analysis for the genetic linkage in the families with non-syndromic recessive deafness. Selected markers had an average heterozygosity of more that 70%. Genotyping of these markers was performed as described above.

Linkage to DFNB1 Locus (Connexin 26)

To test the linkage at DFNB1 locus from linkage, two approaches were followed:

- Linkage of the families to DFNB1 locus was investigated by typing the microsatellite markers (D13S250, D13S175, D13S787, D13S292) mapped in the linkage interval of the locus.
- For mutation screening in the *GJB2* gene at DFNB1, genomic DNA of an affected individual was used. Exon 2 of *GJB2* gene, containing the entire open reading frame of 681 bp encoding 226 amino acids, amplified by two sets of overlapping primers (Table 2.2) and sequenced in an Automated Genetic Analyzer ABI Prism 310® (Applied Biosystem, USA).

The families were also tested for linkage by using microsatellite markers tightly linked to other loci associated with hearing impairment including DFNB2, DFNB3, DFNB4, DFNB6, DFNB8/10, DFNB7/11, DFNB12, DFNB16, DFNB18, DFNB21, DFNB24, DFNB29, DFNB31, DFNB36, and DFNB49. Detail of the microsatellite markers used in testing linkage to these loci is given in the Table 2.1.

Polymerase Chain Reaction (PCR)

PCR amplification of the microsatellite markers was performed in 0.2 ml tubes (Axygen, USA) according to standard procedures in a total volume of 25 ul reaction mixture. The reaction was prepared by adding 1 µl (40 ng) genomic DNA, 0.3 µl (20 p mol) of each forward and reversed primer, 0.5 µl deoxyribonucleotide triphosphate (dNTPs, 10 mM), 1.5 µl $MgCl_2$ (25 mM), 0.3 µl (1 U) Taq DNA polymerase (MBI Fermentas, Sunderland, UK), and 2.5 µl 10 X PCR buffer (100 mM Tris-HCl, pH 8.3, 500 mM KCl) (MBI Fermentas, UK) in 20.1 µl PCR water. The reaction mixture was vortexed and centrifuge for few seconds for thorough mixing. The reaction mixture was taken through thermocycling conditions consisting: 5 minutes of 95°C for template DNA denaturation followed by 40 cycles of amplification each consisting of 3 steps: one minute at 95°C for DNA denaturation into single strands; 1 minute at 57°C for primers to hybridize or "anneal" to their complementary sequences on either side of the target sequence: and one minute at 72°C for Taq DNA polymerase to synthesize any unextended strands left. PCR was carried out in Gene Amp PCR system 9600 (Perkin Elmer, USA) and T3 thrmocyclers (Biometra, Germany).

Agarose Gel Electrophoresis

Amplified PCR products were analyzed on 1-2% agarose gel, which was prepared by melting 1 g of agarose in 50 ml 1X TBE buffer (0.89 M Tris, 0.025 M Borate, EDTA pH 8.3), in a microwave oven for two minutes. Ethidium bromide (final concentration 0.5 µg/ml) was added to the gel to facilitate visualization of DNA after electrophoresis. PCR reaction products were mixed with loading dye (0.25% Bromophenol Blue in 40% sucrose solution) and loaded into the wells. Electrophoresis was performed at 100 volts for half an hour in 1 X TBE buffer. Amplified products were detected by placing the gel on UV Transilluminator (Biometra, Germany).

Polyacrylamide Gel Electrophoresis

The amplified PCR products were resolved on 8% non-denaturing polyacrylamide gel. Reagents were mixed in a conical flask and polyacrylamide gel solution was poured between two glass plates held apart by spacers of 1.5 mm thickness. After inserting the comb, gel was allowed to polymerize for 45-60 minutes at room temperature. Amplified products were mixed with loading dye (0.25% bromophenol blue prepared in 40% sucrose solution) and loaded into the wells. Electrophoresis was carried out at 100 volts (30 mA) for 90-100 minutes depending upon the size of amplified length. The gel was stained with ethidium bromide (10 mg/ml) solution for visualization on UV Transilluminator. Gel was photographed by using Digital camera DC 120 (Kodak, USA).

Composition of 8% Polyacrylamide Gel

13.5 ml 30% Acrylamide solution (29 g acrylamide, 1g NN'-Methylene-bisacrylamide).

5 ml 10X TBE

0.35 ml 10% Ammonium persulphate

17.5 µl TEMED (N, N, N, N'-Tetra Methyl Ethylene Diamine)

31.13 ml distilled water

DNA Sequencing

To screen for mutations in exon 2 of *GJB2* gene of family 'A', 'B' and 'C' and *TMC1* gene of family 'C', all exons and splice junctions were PCR amplified from genomic DNA. Primer3 software (Rozen and Skaletsky, 2000) was used to design primers from the intronic sequences of these genes. The primer sequences, their amplified products and the annealing temperatures are described in Tables 2.2-2.3. Amplification reaction was carried out using 40 ng of genomic DNA in a 35 cycles PCR, in which initial 5 min denaturation of template DNA at 95°C was followed by 35 cycles of 95°C for 1 min, 53-62°C for 1 min, and 72°C for 1 min, followed by a final extension at 72°C for 10 min in a volume of 50 µl containing 10 mM Tris-HCl, pH 8.3, 50 mM KCl, 0.2 mM of each dNTP, 1.5 mM $MgCl_2$, 0.5 µM of each primer and 1.0 unit of *Taq* DNA polymerase. PCR products were purified using Rapid PCR Purification kit (Marligen, USA). 300 µl of binding solution (H1) (concentrated

Guanidine HCl, EDTA, Tris-HCl, and Isopropanol) was added to the amplification reaction and mixture was applied to a spin cartridge containing silica-based membranes where the double stranded DNA was selectively adsorbed. Adsorption to the membrane is influenced by buffer composition and temperature. DNA polymerases, buffer, unreacted primers and dNTPs were removed with 500 µl of alcohol-containing wash buffer (H2) (NaCl, EDTA, Tris-HCl). DNA was eluted in Tris-EDTA buffer (10 mM Tris-HCl (pH 8.0), 0.1 mM EDTA) at 65°C. The purified PCR products were subjected to cycle sequencing using Big Dye Terminator version 3.1 ready reaction mix and sequencing buffer (PE Applied Biosystems, Foster city, CA, USA). The reaction mixture was taken through thermocycling conditions consisting: 1 minute of 95°C for template DNA denaturation followed by 30 cycles of amplification each consisting of 3 steps: 30 seconds at 95°C for DNA denaturation; 30 seconds at 53-62°C for primer annealing and 4 minutes at 72°C for extension of complementary DNA strands from primer, final 10 minutes at 72°C for polymerase enzyme to synthesize any unextended strands left.

The sequencing products were purified by ethanol precipitation protocol (POP6 Protocol). Sequencing product was transferred to 1.5 ml microcentrifuge tube, containing 16 µl of distilled water and 64 µl 100% ethanol. Tubes were kept at room temperature for 15 minutes, and centrifuged at 14,000 rpm for 20 minutes. Supernatant was removed and 250 µl of 70% ethanol was added into the tubes. After thorough mixing, tubes were centrifuged at 13,000 rpm for 10 minutes. Supernatant was discarded, and 20 µl of HDF (Hi Di Formamide) was added into the tube, and were placed in 0.5 ml septa tubes to be directly sequenced in an ABI Prism 310 Genetic Analyzer (Applera, Foster City, CA, USA).

Sequence variants were identified via Bioedit sequence alignment editor, version 6.0.7. When a potentially functional sequence variant was found, the exon in which the variant was found was sequenced in all other family members for whom DNA was available. When the identified sequence variant was shown to segregate with the disease status within a family, a minimum 100 unrelated ethnically matched control individuals were also screened for the same exon.

Table 2.1: List of microsatellite markers used for linkage to known DFNB loci

Locus	Candidate Genes	Chromosomal Location	Markers	Distance (cM)*	Polymorphism
DFNB1	*GJB2*	13q12	D13S250	2.9	TNR
			D13S175	2.9	DNR
			D13S633	2.9	TNR
			D13S1275	7.38	DNR
			D13S787	8.02	TNR
			D13S292	8.2	DNR
DFNB2	*MYO7A*	11p13.5	D11S4081	85.51	DNR
			D11S906	88.12	DNR
			D11S911	88.23	DNR
			D11S937	88.32	DNR
			D11S2002	91.48	TNR
DFNB3	*MYO15A*	17p11.2	D17S2196	50.99	Unknown variation
			D17S1871	53.55	DNR
			D17S1824	55.21	DNR
			D17S783	54.41	DNR
DFNB4	*SLC26A4*	7q31	D7S501	117.34	DNR
			D7S496	117.99	DNR
			D7S2459	118.18	DNR
			D7S 692	119.61	DNR
			D7S2418	121.25	DNR
DFNB6	*TMIE*	3p14-21	D3S2319	70.93	TNR
			D3S1767	74.49	DNR
			D3S3647	72.02	DNR
			D3S3582	74.08	DNR
DFNB7/11	*TMC1*	9q13-21	D9S301	68.13	TNR
			D9S1876	69.40	DNR
			D9S1806	68.39	DNR
			D9S175	71.93	DNR
			D9S1122	75.87	TNR
DFNB8/10	*TMPRSS3*	21q22	D21S1260	55.54	DNR
			D21S212	58.54	DNR
			D21S1259	63.04	DNR
			D21S1411	61.33	TNR
			D21S1912	63.83	DNR
			D21S1575		DNR
DFNB12	*CDH23*	10q21-22	D10S1688	89.34	DNR
			D10S1432	93.70	TNR
			D10S535	93.70	DNR
			D10S580	95.51	DNR
			D10S201	99.44	DNR
DFNB16	*STRC*	15q21-22	D15S1044	38.97	DNR
			D15S659	43.74	TNR
			D15S132	45.29	DNR

			D15S978	47.92	DNR
DFNB18	*USH1C*	11p14-15.1	D11S1307	27.88	DNR
			D11S902	30.69	DNR
			D11S2368	33.91	TNR
DFNB21	*TECTA*	11q	D11S1356	126.65	DNR
			D11S4171	128.16	DNR
			D11S925	130.70	DNR
			D11S4464	136.99	TNR
			D11S4110	142.99	DNR
DFNB24	*UNKNOWN*	11p23	D11S4120	106.3	DNR
			D11S876	108.77	DNR
			D11S2000	111.71	TNR
			D11S2017	112.89	TNR
			D11S908	122.22	DNR
			D11S1992	122.22	TriNR
DFNB29	*CLDN14*	21q22	D21S167	44.92	DNR
			D21S1440	45.42	TriNR
			D21S1917	46.52	DNR
			D21S1255	46.79	DNR
			D21S1246	49.49	TNR
			D21S168	49.49	DNR
DFNB31	*WHRN*	9q32-34	D9S302	123.33	TNR
			D9S1776	123.33	DNR
			D9S1872	128.65	DNR
			D9S1881	135.52	DNR
DFNB36	*ESPN*	1p36.3	D1S468	8.76	DNR
			D1S2870	14.04	DNR
			D1S214	14.04	DNR
			D1S2660	14.75	DNR
DFNB49	*UNKNOWN*	5q12.3-14.1	D5S2500	74.39	TNR
			D5S1359		DNR
			D5S647	78.83	DNR
			D5S2003	87.39	DNR
			D5S2041	90.73	DNR

cM: centiMorgan

*-Average-sex distance in cM according to Rutgers combined linkage-physical human genome map (Kong *et al.*, 2004).

Table 2.2: Primers sequences used in screening of *GJB2* gene exon 2

Exon (*GJB2*)			
PRIMER (5′→3′)		Product Size *(bp)	Annealing Temperature (°C)
Forward	**Reverse**		
GTAAGAGTTGGTGTTTGCTC	GATGACCCGGAAGAAGATGC	576	55
CAGCTGATCTTCGTGTCCAC	GAGTTTCACCTGAGGCCTAC	600	57

Table 2.3: Sequences of primers used in screening *TMC1* gene

Exon No.	PRIMER (5′→3′)		Product Size *(bp)	Annealing Temp (°C)
	Forward	**Reverse**		
5	GTTTCAGATGGTGAAATGGC	GGTGGAGAGATATTAAACCC	362	57
6	GCTGGCATTGTATAAGATG	CACACTTCTGCTTACATATC	340	55
7	CATCACGATGTGGAGAATTG	GCATCATCAGATTAAGGCTC	430	57
8	GCTTATGGGTCCTAATGTTG	CCAGTCTCTCTAGTGATAAG	558	55
9	GAAATACAGTCTAGGTTCAC	GCTAAAGTCACACAAGTAAG	486	55
10	GCCAGAGAGACATTTCCAAG	CTTCACAGTGACGAAAGCAG	367	55
11	CCAATGCCTCACAATTAATG	CTCTAAGACGTGAAAATAGC	328	55
12	GGATTTAGTAGTCGATTCCC	CTTAAGACATTCAGCCTGAC	359	57
13	GCAAAACAATAGGGCTCATG	CTCTTACAGACTCTGTTTCC	407	57
14	GCTTCTCCACTTCAACACTC	GATCTTGGTAGGCAGAAACC	370	57
15	CACCTGGTTTGTGGAATCTC	GCTTGGTTAACTGTAAGGGC	489	57
16	ACACACACTCAGTCACATGC	CATACACTTCTGTTGGTGGC	429	54
17	GTTTCTGGATTGTCCTTGCC	AATTCAGAGCCAGCACACAG	425	55
18	TGCAGTCTTCAAGCCAATAC	AACCAGAGACCTTTGTTCAC	395	55
19	CTATTGTTGCTGAAGGGAAG	ACACCGATTGTATTCTCCTC	284	57
20	CTGGTTGAAAGTGGCAGTGT	GGATCTCATTTCCACCAACC	495	57
21	AAGTGTCAGCAAGTTGTAGC	AATTTTAGCCTCTCTCCACC	431	54
22/23	TCTCTTTACCTCTCTGGACC	TCGCTCACAGCAATAATGCC	480	57
24	AATACAGATTTCTGGCCACC	AAATAGCAGTTCCACAGTGC	255	57

*base pair

Results

RESULTS

Pedigree Analysis

Family 'A'

The family 'A' resides in Dera Ghazi Khan of Punjab province. The family history presented in the pedigree contains four generations (Figure 3.1). Seven individuals in the family are affected including three males (III-4, III-5 and IV-8) and four females (IV-6, IV-7, IV-10 and IV-11). The pedigree analysis shows that the affected individuals being produced by the unaffected parents and the trait appears independent of the sex suggest that the trait is transmitted in autosomal recessive manner. After a general examination and interviews regarding the complete medical history of the individuals and family relationships it was concluded that there was no possibility of the environmental factors and infections to be the cause of deafness. The affected persons are deaf and mute since birth. Blood samples were collected from all the participating members of the family including five normal (III-1, III-3, IV-3, IV-4 and IV-5) and four affected (IV-6, IV-7, IV-8 and IV-10) and then processed for DNA extraction.

Family 'B'

The family 'B' resides in Multan in Punjab province. The family data shows that family consists of five generations (Figure 3.2). Six individuals including two males (IV-1 and IV-6) and four females (IV-3, IV-4, V-1 and V-3) are affected with prelingual nonsyndromic hearing impairment. The affected individuals, regardless of age, display the same level of profound hearing impairment implying that deafness is not progressive. There is no evidence that the hearing impairment in the kindred belongs to any syndrome and also no external ear abnormalities were observed in any of the affected individuals. The fact that affected individuals are being produced by the unaffected parents and the trait appearing in both the sexes suggest that the trait is transmitted in autosomal recessive manner.

The DNA extracted from the blood samples collected from nine individuals of the family including five affected (IV-1, IV-4, IV-6, V-1 and V-3) and four normal (III-5, IV-5, IV-7 and V-2).

Family 'C'

The family 'C' resides in Multan. The family pedigree presented in the Figure 3.3, shows that family consists of four generations. Two females (IV-2 and IV-3) are affected by prelingual nonsyndromic hearing impairment. The affected individuals use sign language for communication. All the affected individuals, regardless of age, display the same level of profound hearing impairment implying that deafness is not progressive. There is no evidence that the hearing impairment in the kindred belongs to any syndrome and also no external ear abnormalities were observed in any of the affected individuals. The fact that affected individuals are being produced by the unaffected parents and the trait appearing in both the sexes suggest that the trait is transmitted in autosomal recessive manner.

The DNA was extracted from the blood samples collected from three individuals of the family including two affected (IV-2 and IV-3) and one normal (IV-1).

Genetic Mapping of Candidate Genes for Autosomal Recessive Nonsyndromic Deafness

Seventy one candidate gene loci (DFNB) for autosomal recessive nonsyndromic deafness have been identified so far. In linkage studies it is important that some candidate intervals should be tested for linkage or exclusion before performing genome-wide search. In the present study, three families (A, B and C) were tested for the linkage to several known DFNB loci. Table 2.1 summarizes the microsatellite markers in the region of known loci, which were used in the present study for candidate gene mapping. Average heterozygosity of the selected markers is greater than 70%. Analysis of microsatellite markers was carried out by using a standard PCR reaction and electrophoresis in 8% non-denaturing polyacrylamide gel. Microsatellite markers were visualized by staining the gel with ethidium bromide and genotypes were assigned by visual inspection.

In the family 'A' (Figure 3.1) six DNA samples including four affected (IV-6, IV-7, IV-8 and IV-10) and two normal (III-3 and IV-5) were selected for genotyping the markers linked to the candidate genes. From the analysis of the results obtained with polymorphic microsatellite markers specific for the DFNB1 (Figure 3.4, 3.5), it was evident that all the affected individuals were heterozygous for different combinations of the parental alleles thus excluding family 'A' from linkage to DFNB1 locus. In order to verify the results obtained with DFNB1 linked markers, *GJB2* gene (Kelsell *et al.*, 1997) implicated earlier

in causing deafness at this locus (Guilford *et al.*, 1994), was sequenced in one affected individual (IV-6) of family 'A'. Sequence analysis of coding exon 2 of *GJB2* gene in the affected individual showed wild type sequence. This further supported the exclusion of family 'A' from linkage to DFNB1 locus.

In family 'A' several other deafness loci including DFNB49 (Figure 3.6, 3.7), DFNB24 (Figure 3.8, 3.9), DFNB6 (Figure 3.10, 3.11), DFNB7/11 (Figure 3.12, 3.13), DFNB18 (Figure 3.14, 3.15), DFNB31 (Figure 3.16, 3.17), DFNB36 (Figure 3.18, 3.19), DFNB2 (Figure 3.20, 3.21), DFNB3 (Figure 3.22, 3.23), DFNB4 (Figure 3.24, 3.25), DFNB8/10 (Figure 3.26, 3.27), DFNB12 (Figure 3.28, 3.29), DFNB16 (Figure 3.30, 3.31), DFNB21 (Figure 3.32, 3.33) and DFNB29 (Figure 3.34, 3.35) were tested for linkage. Analyses of the results indicate that family 'A' was not linked to any of these loci.

In the family 'B' (Figure 3.2) seven DNA samples including five affected (IV-1, IV-6, IV-4, V-1 and V-3) and two normal (IV-7 and V-2) were selected for genotyping the markers linked to the candidate genes. It is evident from the analysis of the results obtained with the microsatellite markers specific for the DFNB1 locus (Figure 3.36, 3.37) that most of the kindred showed heterozygous pattern for the different combinations of the parenatal alleles thus excluding the linkage in family 'B' to DFNB1 locus. In order to verify results obtained with DFNB1 linked markers, *GJB2* gene was sequenced in one affected individual (V-3) of the family 'B'. Sequence analysis of coding exon 2 of *GJB2* gene in the affected individual showed wild type sequence. This further supported the exclusion of family 'B' from linkage to DFNB1 locus.

In family 'B' several other deafness loci including DFNB49 (Figure 3.38, 3.39), DFNB24 (Figure 3.40, 3.41), DFNB6 (Figure 3.42, 3.43), DFNB7/11 (Figure 3.44, 3.45), DFNB18 (Figure 3.46, 3.47), DFNB31 (Figure 3.48, 3.49), DFNB36 (Figure 3.50, 3.51), DFNB2 (Figure 3.52, 3.53), DFNB3 (Figure 3.54, 3.55), DFNB4 (Figure 3.56, 3.57), DFNB8/10 (Figure 3.58, 3.59), DFNB12 (Figure 3.60, 3.61), DFNB16 (Figure 3.62, 3.63), DFNB21 (Figure 3.64, 3.65) and DFNB29 (Figure 3.66, 3.67) were tested for linkage. Analyses of the results indicate that family 'B' was not linked to any of these loci.

In the family 'C' (Figure 3.3) three DNA samples including two affected (IV-2 and IV-3) and one normal (IV-1) were selected for genotyping the markers linked to the candidate genes. It is evident from the analysis of the results obtained with the microsatellite

markers specific for the DFNB1 locus (Figure 3.68, 3.69) that all of the kindred showed heterozygous pattern for the different combinations of the parenatal alleles thus excluding the linkage in family 'C' to DFNB1 locus. In order to verify results obtained with DFNB1 linked markers, *GJB2* gene was sequenced in one affected individual (IV-2) of the family 'C'. Sequence analysis of coding exon 2 of *GJB2* gene in the affected individual (IV-2) showed wild type sequence. This further supported the exclusion of family 'C' from linkage to DFNB1 locus.

In family 'C' several other deafness loci including DFNB49 (Figure 3.70, 3.71), DFNB24 (Figure 3.72, 3.73), DFNB6 (Figure 3.74, 3.75) and DFNB7/11 (Figure 3.76, 3.77), were genotyped. Genotyping of three members of the family C including 2 affected individuals (IV-2 and IV-3) was carried out by using polymorphic microsatellite markers D9S301, D9S1806, D9S1876, D9S175, which are closely linked to DFNB7/11 locus (*TMC1* gene). The markers were fully informative (Figure 3.76-3.80) and 2 affected members of the family were homozygous and a normal individual was heterozygous for these four markers, suggesting linkage to the DFNB7/11 locus on chromosome 9q13-21.

In family C, which showed linkage to DFNB7/11 locus on chromosome 9q13-21, a candidate gene *TMC1* within linkage interval was screened in an affected individual. Sequence analysis of all the 24 exons and splice junctions of *TMC1* gene failed to identify any functional sequence variant, suggesting that probably the mutation is present in the regulatory sequence.

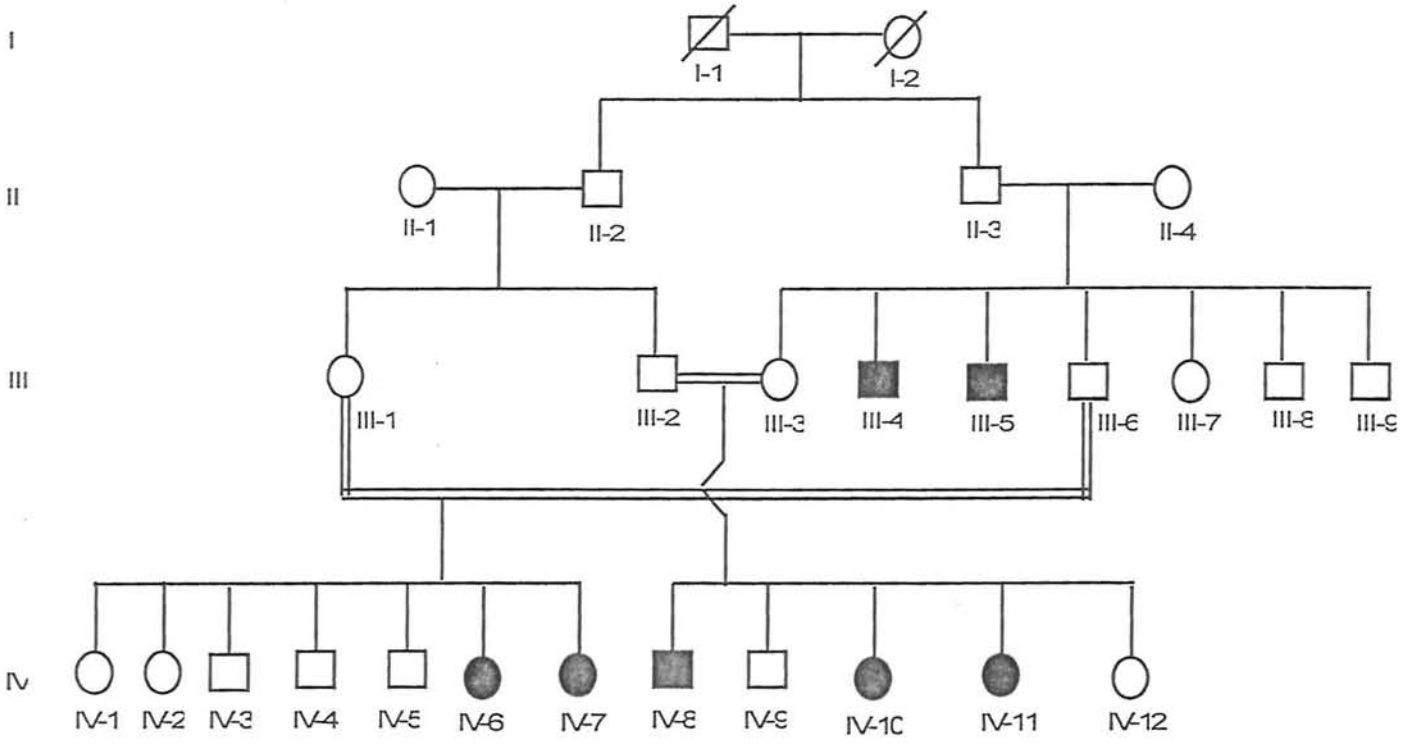

Figure3.1. Pedigree of family 'A' with non-syndromic hearing loss in which the squares represent males and circle females. Filled squares and circles represent affected individuals. Double lines indicate family inter marriages. Cross lines on the squares and circles indicate deceased individuals.

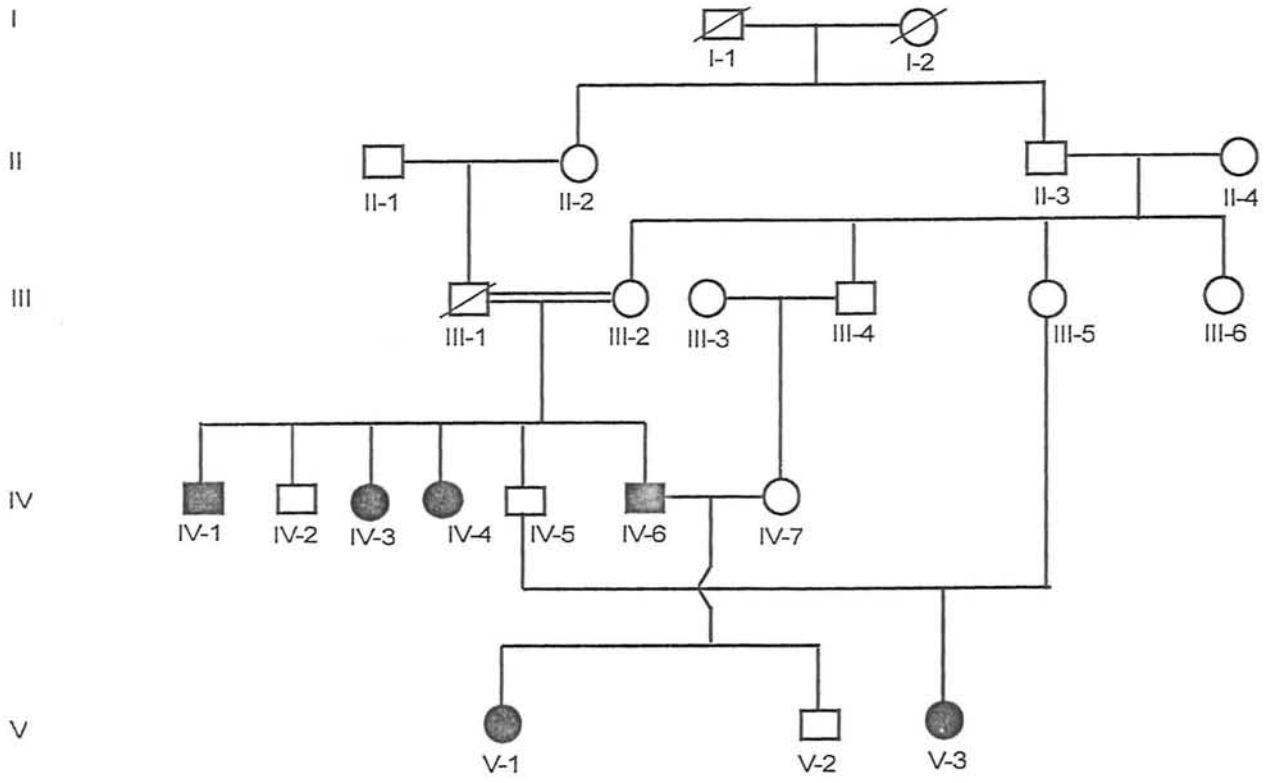

Figure 3.2 Pedigree of family 'B' with non-syndromic hearing loss in which the squares represent males and cirle females. Filled squares and cirles represent affected individuals. Double lines indicate family inter marriages. Cross lines on the squares and circles indicate deceased individuals.

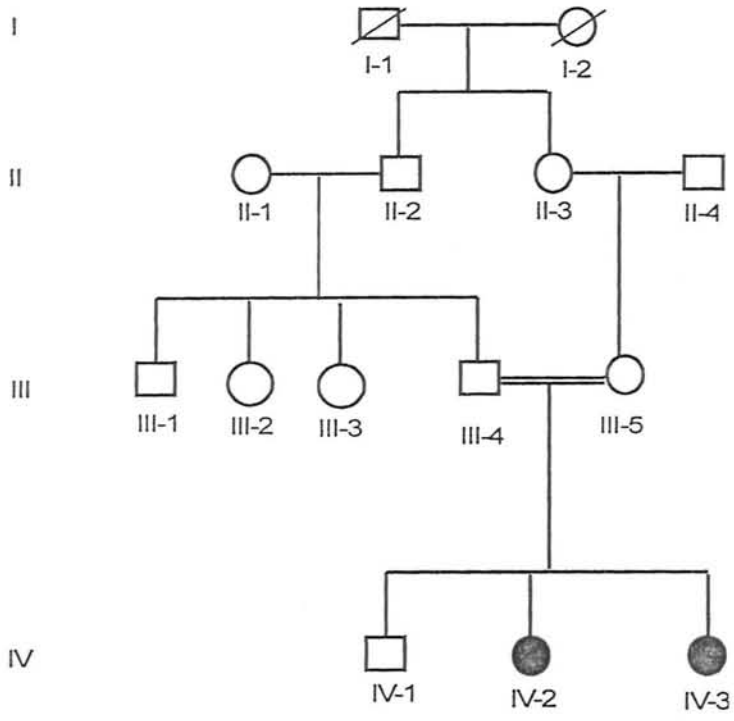

Figure 3.3. Pedigree of family 'C' with non-syndromic hearing loss in which the squares represent males and circle females. Filled squares and circles represent affected individuals. Double lines indicate family inter marriages. Cross lines on the squares and circles indicate deceased individuals.

Family A

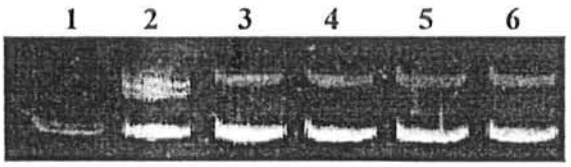

1	IV-7	Affected	4	IV-10	Affected
2	IV-6	Affected	5	IV-3	Normal
3	IV-8	Affected	6	III-3	Normal

Figure 3.4 Electropherogram of ethidium bromide stained 8% non-denaturing polyacrylamide gel showing allele pattern obtained with marker D13S250 at 2.9 cM, linked to DFNB1 on chromosome 13q12. The Roman with Arabic numerals refers to the individuals in the pedigree.

Family A

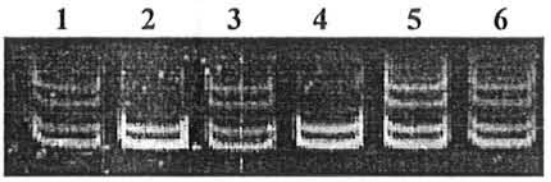

1	IV-7	Affected	4	IV-10	Affected
2	IV-6	Affected	5	IV-3	Normal
3	IV-8	Affected	6	III-3	Normal

Figure 3.5 Electropherogram of ethidium bromide stained 8% non-denaturing polyacrylamide gel showing allele pattern obtained with marker D13S292 at 8.02 cM, linked to DFNB1 on chromosome 13q12. The Roman with Arabic numerals refers to the individuals in the pedigree.

Family A

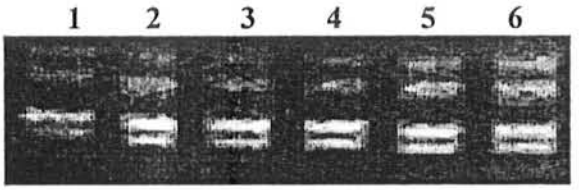

1	IV-7	Affected	4	IV-10	Affected
2	IV-6	Affected	5	IV-3	Normal
3	IV-8	Affected	6	III-3	Normal

Figure 3.6 Electropherogram of ethidium bromide stained 8% non-denaturing polyacrylamide gel showing allele pattern obtained with marker D5S647 at 78.83 cM, linked to DFNB49 on chromosome 5q12.3-14.1. The Roman with Arabic numerals refers to the individuals in the pedigree.

Family A

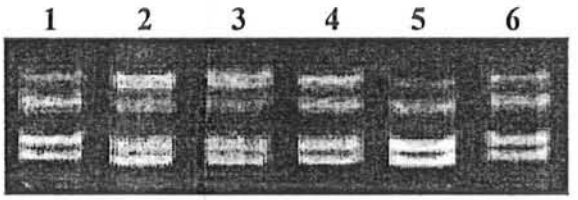

1	IV-7	Affected	4	IV-10	Affected
2	IV-6	Affected	5	IV-3	Normal
3	IV-8	Affected	6	III-3	Normal

Figure 3.7 Electropherogram of ethidium bromide stained 8% non-denaturing polyacrylamide gel showing allele pattern obtained with marker D5S2003 at 87.39 cM, linked to DFNB49 on chromosome 5q12.3-14.1. The Roman with Arabic numerals refers to the individuals in the pedigree.

Family A

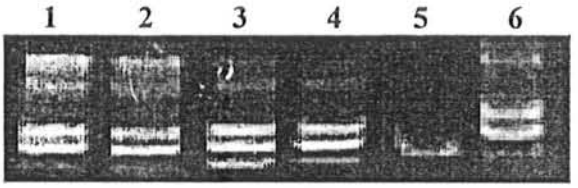

1	IV-7	Affected	4	IV-10	Affected
2	IV-6	Affected	5	IV-3	Normal
3	IV-8	Affected	6	III-3	Normal

Figure 3.8 Electropherogram of ethidium bromide stained 8% non-denaturing polyacrylamide gel showing allele pattern obtained with marker D11S4120 at 106.3 cM, linked to DFNB24 on chromosome 11q23. The Roman with Arabic numerals refers to the individuals in the pedigree.

Family A

1	IV-7	Affected	4	IV-10	Affected
2	IV-6	Affected	5	IV-3	Normal
3	IV-8	Affected	6	III-3	Normal

Figure 3.9 Electropherogram of ethidium bromide stained 8% non-denaturing polyacrylamide gel showing allele pattern obtained with marker D11S2017 at 112.789cM, linked to DFNB24 on chromosome 11q23. The Roman with Arabic numerals refers to the individuals in the pedigree.

Family A

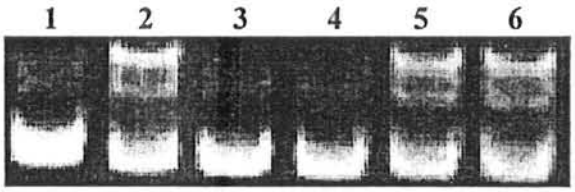

1	IV-7	Affected	4	IV-10	Affected
2	IV-6	Affected	5	IV-3	Normal
3	IV-8	Affected	6	III-3	Normal

Figure 3.10 Electropherogram of ethidium bromide stained 8% non-denaturing polyacrylamide gel showing allele pattern obtained with marker D3S2319 at 70.93 cM, linked to DFNB6 on chromosome 3p14-21. The Roman with Arabic numerals refers to the individuals in the pedigree.

Family A

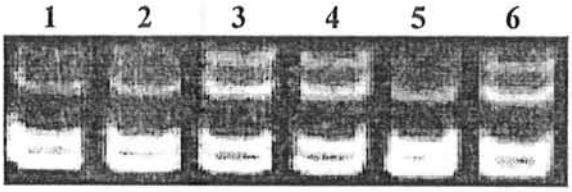

1	IV-7	Affected	4	IV-10	Affected
2	IV-6	Affected	5	IV-3	Normal
3	IV-8	Affected	6	III-3	Normal

Figure 3.11 Electropherogram of ethidium bromide stained 8% non-denaturing polyacrylamide gel showing allele pattern obtained with marker D3S3582 at 74.08 cM, linked to DFNB6 on chromosome 3p14-21. The Roman with Arabic numerals refers to the individuals in the pedigree.

Family A

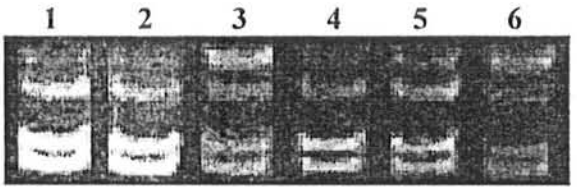

1	IV-7	Affected	4	IV-10	Affected
2	IV-6	Affected	5	IV-3	Normal
3	IV-8	Affected	6	III-3	Normal

Figure 3.12 Electropherogram of ethidium bromide stained 8% non-denaturing polyacrylamide gel showing allele pattern obtained with marker D9S1862 at 66.55 cM, linked to DFNB7 on chromosome 9q13-21. The Roman with Arabic numerals refers to the individuals in the pedigree.

Family A

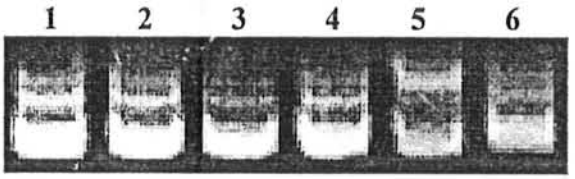

1	IV-7	Affected	4	IV-10	Affected
2	IV-6	Affected	5	IV-3	Normal
3	IV-8	Affected	6	III-3	Normal

Figure 3.13 Electropherogram of ethidium bromide stained 8% non-denaturing polyacrylamide gel showing allele pattern obtained with marker D9S1806 at 68.39 cM, linked to DFNB7 on chromosome 9q13-21. The Roman with Arabic numerals refers to the individuals in the pedigree.

Family A

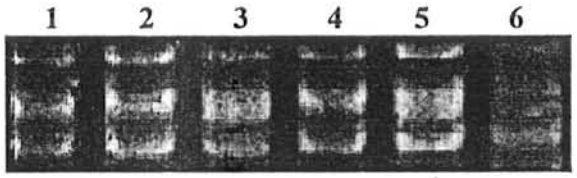

1	IV-7	Affected	4	IV-10	Affected
2	IV-6	Affected	5	IV-3	Normal
3	IV-8	Affected	6	III-3	Normal

Figure 3.14 Electropherogram of ethidium bromide stained 8% non-denaturing polyacrylamide gel showing allele pattern obtained with marker D11S902 at 30.69 cM, linked to DFNB18 on chromosome 11p14-15.1. The Roman with Arabic numerals refers to the individuals in the pedigree.

Family A

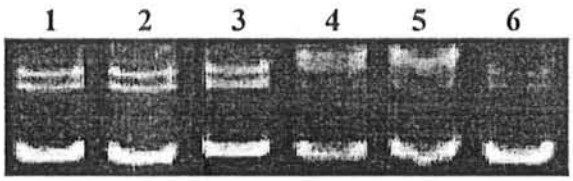

1	IV-7	Affected	4	IV-10	Affected
2	IV-6	Affected	5	IV-3	Normal
3	IV-8	Affected	6	III-3	Normal

Figure 3.15 Electropherogram of ethidium bromide stained 8% non-denaturing polyacrylamide gel showing allele pattern obtained with marker D11S2368 at 33.91 cM, linked to DFNB18 on chromosome 11p14-15.1. The Roman with Arabic numerals refers to the individuals in the pedigree.

Family A

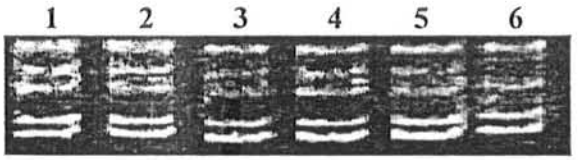

1	IV-7	Affected	4	IV-10	Affected
2	IV-6	Affected	5	IV-3	Normal
3	IV-8	Affected	6	III-3	Normal

Figure 3.16 Electropherogram of ethidium bromide stained 8% non-denaturing polyacrylamide gel showing allele pattern obtained with marker D9S302 at 123.79 cM, linked to DFNB31 on chromosome 9q32-34. The Roman with Arabic numerals refers to the individuals in the pedigree.

Family A

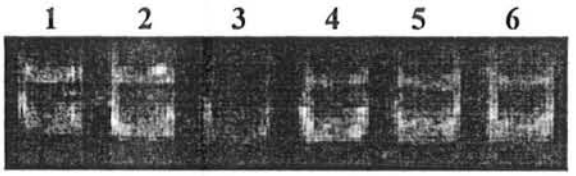

1	IV-7	Affected	4	IV-10	Affected
2	IV-6	Affected	5	IV-3	Normal
3	IV-8	Affected	6	III-3	Normal

Figure 3.17 Electropherogram of ethidium bromide stained 8% non-denaturing polyacrylamide gel showing allele pattern obtained with marker D9S1872 at 128.65 cM, linked to DFNB31 on chromosome 9q32-34. The Roman with Arabic numerals refers to the individuals in the pedigree.

Family A

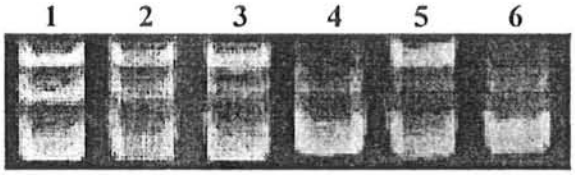

1	IV-7	Affected	4	IV-10	Affected
2	IV-6	Affected	5	IV-3	Normal
3	IV-8	Affected	6	III-3	Normal

Figure 3.18 Electropherogram of ethidium bromide stained 8% non-denaturing polyacrylamide gel showing allele pattern obtained with marker D1S468 at 8.76 cM, linked to DFNB36 on chromosome 1p36.3. The Roman with Arabic numerals refers to the individuals in the pedigree.

Family A

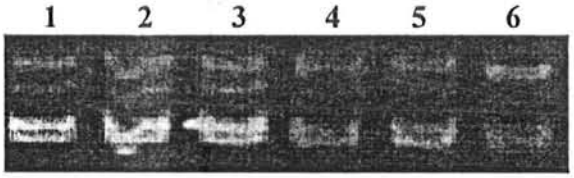

1	IV-7	Affected	4	IV-10	Affected
2	IV-6	Affected	5	IV-3	Normal
3	IV-8	Affected	6	III-3	Normal

Figure 3.19 Electropherogram of ethidium bromide stained 8% non-denaturing polyacrylamide gel showing allele pattern obtained with marker D1S214 at 19.07 cM, linked to DFNB36 on chromosome 1p36.3. The Roman with Arabic numerals refers to the individuals in the pedigree.

Family A

1	IV-7	Affected	4	IV-10	Affected
2	IV-6	Affected	5	IV-3	Normal
3	IV-8	Affected	6	III-3	Normal

Figure 3.20 Electropherogram of ethidium bromide stained 8% non-denaturing polyacrylamide gel showing allele pattern obtained with marker D11S4081 at 85.51 cM, linked to DFNB2 on chromosome 11p13.5. The Roman with Arabic numerals refers to the individuals in the pedigree.

Family A

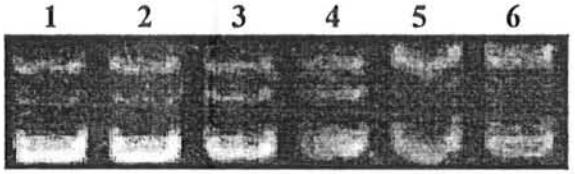

1	IV-7	Affected	4	IV-10	Affected
2	IV-6	Affected	5	IV-3	Normal
3	IV-8	Affected	6	III-3	Normal

Figure 3.21 Electropherogram of ethidium bromide stained 8% non-denaturing polyacrylamide gel showing allele pattern obtained with marker D11S937 at 88.32 cM, linked to DFNB2 on chromosome 11p13.5. The Roman with Arabic numerals refers to the individuals in the pedigree.

Family A

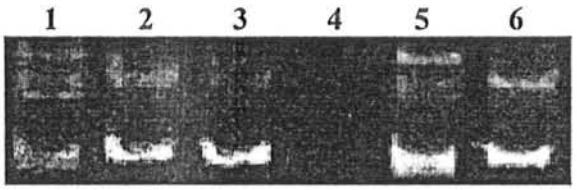

1	IV-7	Affected	4	IV-10	Affected
2	IV-6	Affected	5	IV-3	Normal
3	IV-8	Affected	6	III-3	Normal

Figure 3.22 Electropherogram of ethidium bromide stained 8% non-denaturing polyacrylamide gel showing allele pattern obtained with marker D17S2196 at 50.99 cM, linked to DFNB3 on chromosome 17p11.2. The Roman with Arabic numerals refers to the individuals in the pedigree.

Family A

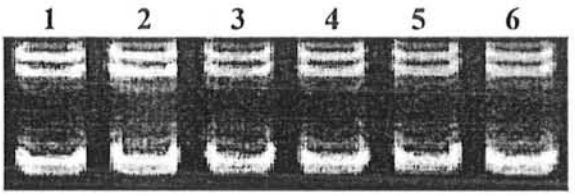

1	IV-7	Affected	4	IV-10	Affected
2	IV-6	Affected	5	IV-3	Normal
3	IV-8	Affected	6	III-3	Normal

Figure 3.23 Electropherogram of ethidium bromide stained 8% non-denaturing polyacrylamide gel showing allele pattern obtained with marker D17S783 at 54.41 cM, linked to DFNB3 on chromosome 17p11.2. The Roman with Arabic numerals refers to the individuals in the pedigree.

Family A

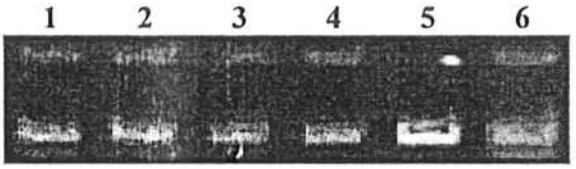

1	IV-7	Affected	4	IV-10	Affected
2	IV-6	Affected	5	IV-3	Normal
3	IV-8	Affected	6	III-3	Normal

Figure 3.24 Electropherogram of ethidium bromide stained 8% non-denaturing polyacrylamide gel showing allele pattern obtained with marker D7S501 at 117.34 cM, linked to DFNB4 on chromosome 7q31. The Roman with Arabic numerals refers to the individuals in the pedigree.

Family A

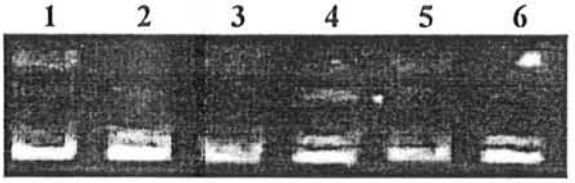

1	IV-7	Affected	4	IV-10	Affected
2	IV-6	Affected	5	IV-3	Normal
3	IV-8	Affected	6	III-3	Normal

Figure 3.25 Electropherogram of ethidium bromide stained 8% non-denaturing polyacrylamide gel showing allele pattern obtained with marker D7S496 at 117.99 cM, linked to DFNB4 on chromosome 7q31. The Roman with Arabic numerals refers to the individuals in the pedigree.

Family A

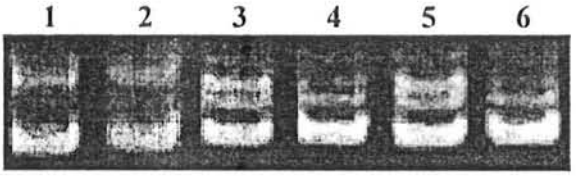

1	IV-7	Affected	4	IV-10	Affected
2	IV-6	Affected	5	IV-3	Normal
3	IV-8	Affected	6	III-3	Normal

Figure 3.26 Electropherogram of ethidium bromide stained 8% non-denaturing polyacrylamide gel showing allele pattern obtained with marker D21S212 at 58.54 cM, linked to DFNB8 on chromosome 21q22. The Roman with Arabic numerals refers to the individuals in the pedigree.

Family A

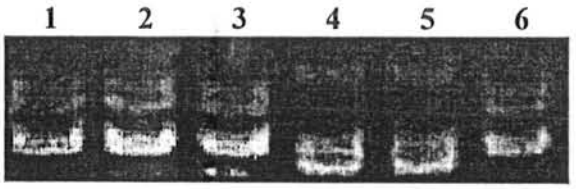

1	IV-7	Affected	4	IV-10	Affected
2	IV-6	Affected	5	IV-3	Normal
3	IV-8	Affected	6	III-3	Normal

Figure 3.27 Electropherogram of ethidium bromide stained 8% non-denaturing polyacrylamide gel showing allele pattern obtained with marker D21S1912 at 68.83 cM, linked to DFNB8 on chromosome 21q22. The Roman with Arabic numerals refers to the individuals in the pedigree.

Family A

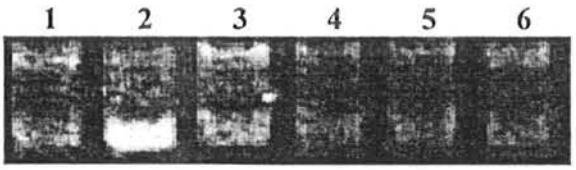

1	IV-7	Affected	4	IV-10	Affected
2	IV-6	Affected	5	IV-3	Normal
3	IV-8	Affected	6	III-3	Normal

Figure 3.28 Electropherogram of ethidium bromide stained 8% non-denaturing polyacrylamide gel showing allele pattern obtained with marker D10S1688 at 89.34 cM, linked to DFNB12 on chromosome 10q21-22. The Roman with Arabic numerals refers to the individuals in the pedigree.

Family A

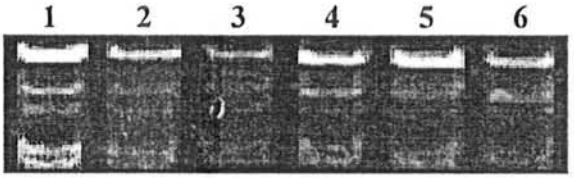

1	IV-7	Affected	4	IV-10	Affected
2	IV-6	Affected	5	IV-3	Normal
3	IV-8	Affected	6	III-3	Normal

Figure 3.29 Electropherogram of ethidium bromide stained 8% non-denaturing polyacrylamide gel showing allele pattern obtained with marker D10S201 at 99.44 cM, linked to DFNB12 on chromosome 10q21-22. The Roman with Arabic numerals refers to the individuals in the pedigree.

Family A

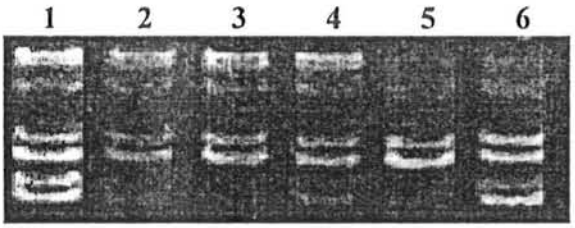

1	IV-7	Affected	4	IV-10	Affected
2	IV-6	Affected	5	IV-3	Normal
3	IV-8	Affected	6	III-3	Normal

Figure 3.30 Electropherogram of ethidium bromide stained 8% non-denaturing polyacrylamide gel showing allele pattern obtained with marker D15S1044 at 38.97 cM, linked to DFNB16 on chromosome 15q21-22. The Roman with Arabic numerals refers to the individuals in the pedigree.

Family A

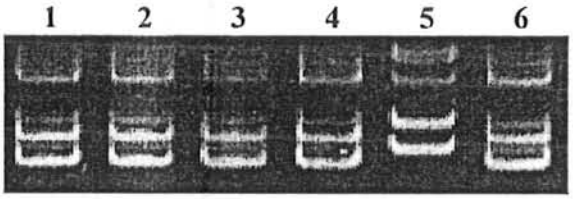

1	IV-7	Affected	4	IV-10	Affected
2	IV-6	Affected	5	IV-3	Normal
3	IV-8	Affected	6	III-3	Normal

Figure 3.31 Electropherogram of ethidium bromide stained 8% non-denaturing polyacrylamide gel showing allele pattern obtained with marker D15S978 at 47.92 cM, linked to DFNB16 on chromosome 15q21-22. The Roman with Arabic numerals refers to the individuals in the pedigree.

Family A

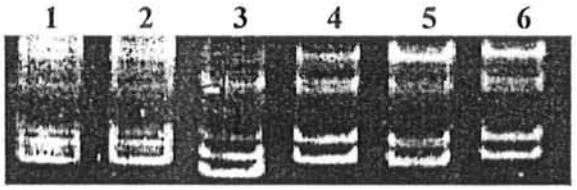

1	IV-7	Affected	4	IV-10	Affected
2	IV-6	Affected	5	IV-3	Normal
3	IV-8	Affected	6	III-3	Normal

Figure 3.32 Electropherogram of ethidium bromide stained 8% non-denaturing polyacrylamide gel showing allele pattern obtained with marker D11S925 at 130.7 cM, linked to DFNB21 on chromosome 11q. The Roman with Arabic numerals refers to the individuals in the pedigree.

Family A

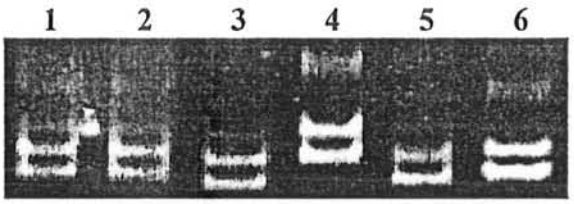

1	IV-7	Affected	4	IV-10	Affected
2	IV-6	Affected	5	IV-3	Normal
3	IV-8	Affected	6	III-3	Normal

Figure 3.33 Electropherogram of ethidium bromide stained 8% non-denaturing polyacrylamide gel showing allele pattern obtained with marker D11S4110 at 142.99 cM, linked to DFNB21 on chromosome 11q. The Roman with Arabic numerals refers to the individuals in the pedigree.

Family A

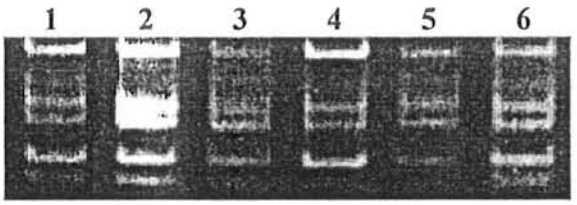

1	IV-7	Affected	4	IV-10	Affected
2	IV-6	Affected	5	IV-3	Normal
3	IV-8	Affected	6	III-3	Normal

Figure 3.34 Electropherogram of ethidium bromide stained 8% non-denaturing polyacrylamide gel showing allele pattern obtained with marker D21S167 at 44.92 cM, linked to DFNB29 on chromosome 21q22. The Roman with Arabic numerals refers to the individuals in the pedigree.

Family A

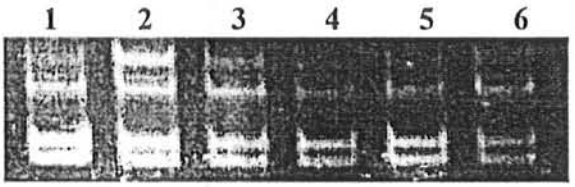

1	IV-7	Affected	4	IV-10	Affected
2	IV-6	Affected	5	IV-3	Normal
3	IV-8	Affected	6	III-3	Normal

Figure 3.35 Electropherogram of ethidium bromide stained 8% non-denaturing polyacrylamide gel showing allele pattern obtained with marker D21S1246 at 49.49 cM, linked to DFNB29 on chromosome 21q22. The Roman with Arabic numerals refers to the individuals in the pedigree.

Family B

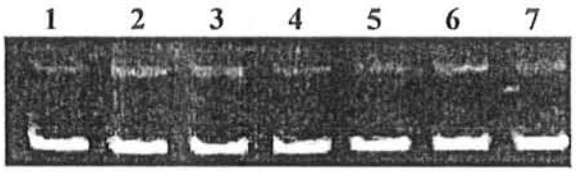

1	IV-1	Affected	4	IV-6	Affected
2	V-1	Affected	5	IV-7	Normal
3	V-3	Affected	6	V-2	Normal
			7	IV-4	Affected

Figure 3.36 Electropherogram of ethidium bromide stained 8% non-denaturing polyacrylamide gel showing allele pattern obtained with marker D13S250 at 2.9 cM, linked to DFNB1 on chromosome 13q12. The Roman with Arabic numerals refers to the individuals in the pedigree.

Family B

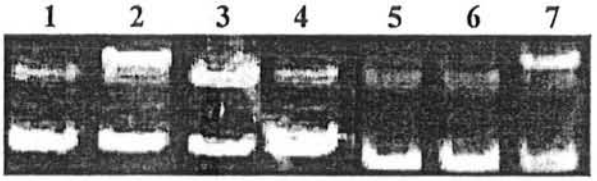

1	IV-1	Affected	4	IV-6	Affected
2	V-1	Affected	5	IV-7	Normal
3	V-3	Affected	6	V-2	Normal
			7	IV-4	Affected

Figure 3.37 Electropherogram of ethidium bromide stained 8% non-denaturing polyacrylamide gel showing allele pattern obtained with marker D13S787 at 8.02 cM, linked to DFNB1 on chromosome 13q12. The Roman with Arabic numerals refers to the individuals in the pedigree.

Family B

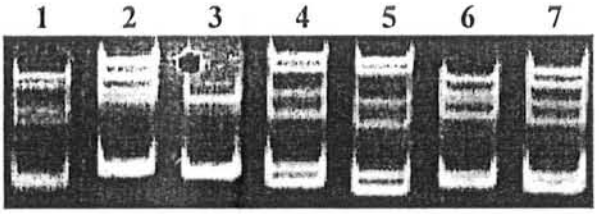

1	IV-1	Affected	4	IV-6	Affected
2	V-1	Affected	5	IV-7	Normal
3	V-3	Affected	6	V-2	Normal
			7	IV-4	Affected

Figure 3.38 Electropherogram of ethidium bromide stained 8% non-denaturing polyacrylamide gel showing allele pattern obtained with marker D5S2500 at 74.39 cM, linked to DFNB49 on chromosome 5q12.3-14.1. The Roman with Arabic numerals refers to the individuals in the pedigree.

Family B

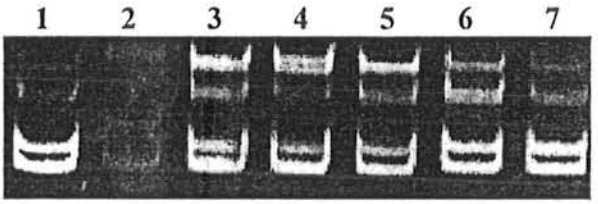

1	IV-1	Affected	4	IV-6	Affected
2	V-1	Affected	5	IV-7	Normal
3	V-3	Affected	6	V-2	Normal
			7	IV-4	Affected

Figure 3.39 Electropherogram of ethidium bromide stained 8% non-denaturing polyacrylamide gel showing allele pattern obtained with marker D5S2003 at 87.39 cM, linked to DFNB49 on chromosome 5q12.3-14.1. The Roman with Arabic numerals refers to the individuals in the pedigree.

Family B

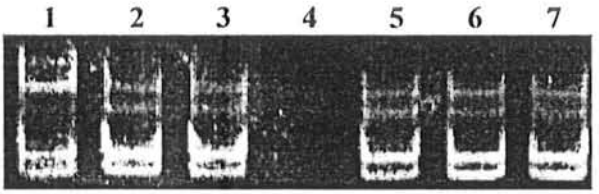

1	IV-1	Affected	4	IV-6	Affected
2	V-1	Affected	5	IV-7	Normal
3	V-3	Affected	6	V-2	Normal
			7	IV-4	Affected

Figure 3.40 Electropherogram of ethidium bromide stained 8% non-denaturing polyacrylamide gel showing allele pattern obtained with marker D11S4120 at 106.3 cM, linked to DFNB24 on chromosome 11q23. The Roman with Arabic numerals refers to the individuals in the pedigree.

Family B

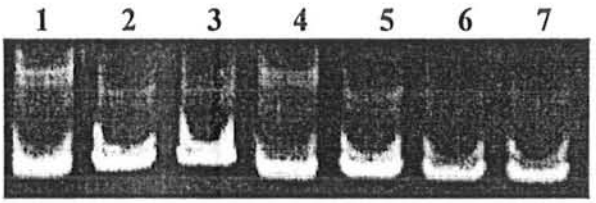

1	IV-1	Affected	4	IV-6	Affected
2	V-1	Affected	5	IV-7	Normal
3	V-3	Affected	6	V-2	Normal
			7	IV-4	Affected

Figure 3.41 Electropherogram of ethidium bromide stained 8% non-denaturing polyacrylamide gel showing allele pattern obtained with marker D11S2017 at 112.89 cM, linked to DFNB24 on chromosome 11q23. The Roman with Arabic numerals refers to the individuals in the pedigree.

Family B

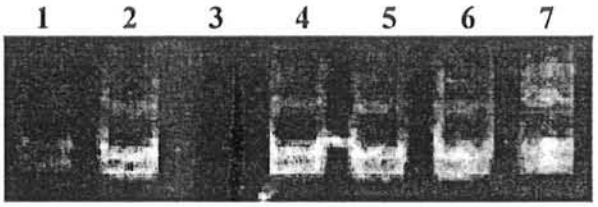

1	IV-1	Affected	4	IV-6	Affected
2	V-1	Affected	5	IV-7	Normal
3	V-3	Affected	6	V-2	Normal
			7	IV-4	Affected

Figure 3.42 Electropherogram of ethidium bromide stained 8% non-denaturing polyacrylamide gel showing allele pattern obtained with marker D3S3647 at 72.02 cM, linked to DFNB6 on chromosome 3p14-21. The Roman with Arabic numerals refers to the individuals in the pedigree.

Family B

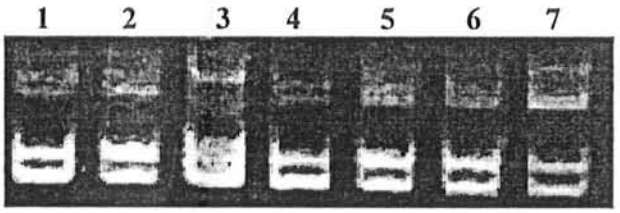

1	IV-1	Affected	4	IV-6	Affected
2	V-1	Affected	5	IV-7	Normal
3	V-3	Affected	6	V-2	Normal
			7	IV-4	Affected

Figure 3.43 Electropherogram of ethidium bromide stained 8% non-denaturing polyacrylamide gel showing allele pattern obtained with marker D3S3582 at 74.08 cM, linked to DFNB6 on chromosome 3p14-21. The Roman with Arabic numerals refers to the individuals in the pedigree.

Family B

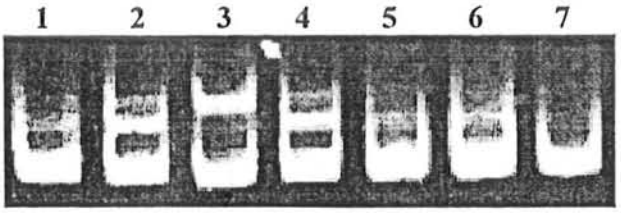

1	IV-1	Affected	4	IV-6	Affected
2	V-1	Affected	5	IV-7	Normal
3	V-3	Affected	6	V-2	Normal
			7	IV-4	Affected

Figure 3.44 Electropherogram of ethidium bromide stained 8% non-denaturing polyacrylamide gel showing allele pattern obtained with marker D9S1806 at 68.39 cM, linked to DFNB7 on chromosome 9p13-21. The Roman with Arabic numerals refers to the individuals in the pedigree.

Family B

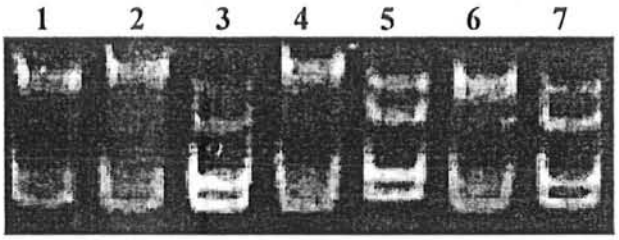

1	IV-1	Affected	4	IV-6	Affected
2	V-1	Affected	5	IV-7	Normal
3	V-3	Affected	6	V-2	Normal
			7	IV-4	Affected

Figure 3.45 Electropherogram of ethidium bromide stained 8% non-denaturing polyacrylamide gel showing allele pattern obtained with marker D9S175 at 71.93 cM, linked to DFNB7 on chromosome 9p13-21. The Roman with Arabic numerals refers to the individuals in the pedigree.

Family B

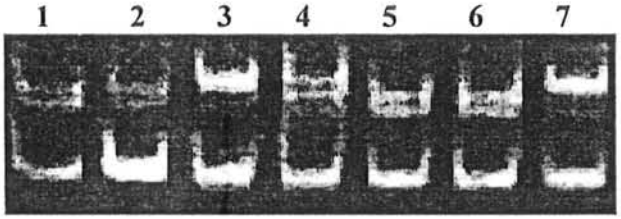

1	IV-1	Affected	4	IV-6	Affected
2	V-1	Affected	5	IV-7	Normal
3	V-3	Affected	6	V-2	Normal
			7	IV-4	Affected

Figure 3.46 Electropherogram of ethidium bromide stained 8% non-denaturing polyacrylamide gel showing allele pattern obtained with marker D11S902 at 30.69 cM, linked to DFNB18 on chromosome 11p14-15.1. The Roman with Arabic numerals refers to the individuals in the pedigree.

Family B

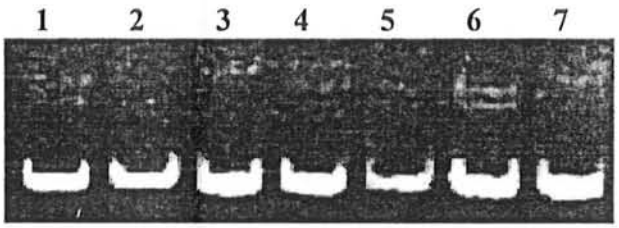

1	IV-1	Affected	4	IV-6	Affected
2	V-1	Affected	5	IV-7	Normal
3	V-3	Affected	6	V-2	Normal
			7	IV-4	Affected

Figure 3.47 Electropherogram of ethidium bromide stained 8% non-denaturing polyacrylamide gel showing allele pattern obtained with marker D11S2368 at 33.91 cM, linked to DFNB18 on chromosome 11p14-15.1. The Roman with Arabic numerals refers to the individuals in the pedigree.

Family B

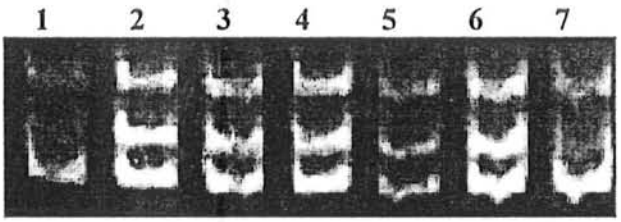

1	IV-1	Affected	4	IV-6	Affected
2	V-1	Affected	5	IV-7	Normal
3	V-3	Affected	6	V-2	Normal
			7	IV-4	Affected

Figure 3.48 Electropherogram of ethidium bromide stained 8% non-denaturing polyacrylamide gel showing allele pattern obtained with marker D9S302 at 123.79 cM, linked to DFNB31 on chromosome 9q32-34. The Roman with Arabic numerals refers to the individuals in the pedigree.

Family B

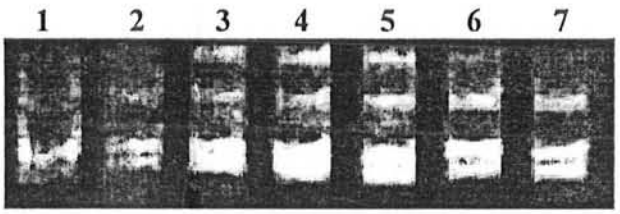

1	IV-1	Affected	4	IV-6	Affected
2	V-1	Affected	5	IV-7	Normal
3	V-3	Affected	6	V-2	Normal
			7	IV-4	Affected

Figure 3.49 Electropherogram of ethidium bromide stained 8% non-denaturing polyacrylamide gel showing allele pattern obtained with marker D9S1872 at 128.65 cM, linked to DFNB31 on chromosome 9q32-34. The Roman with Arabic numerals refers to the individuals in the pedigree.

Family B

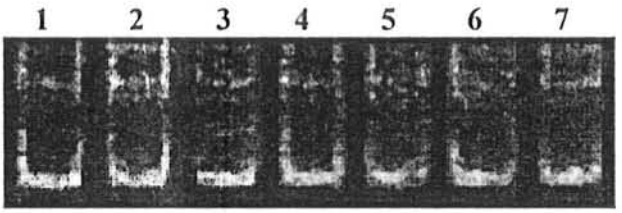

1	IV-1	Affected	4	IV-6	Affected
2	V-1	Affected	5	IV-7	Normal
3	V-3	Affected	6	V-2	Normal
			7	IV-4	Affected

Figure 3.50 Electropherogram of ethidium bromide stained 8% non-denaturing polyacrylamide gel showing allele pattern obtained with marker D1S468 at 8.76 cM, linked to DFNB36 on chromosome 1p36.3. The Roman with Arabic numerals refers to the individuals in the pedigree.

Family B

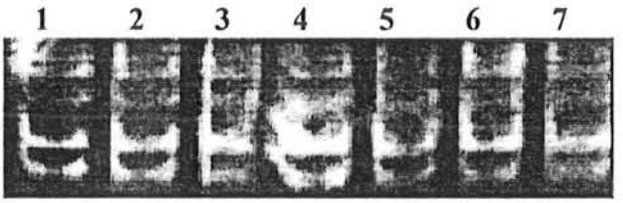

1	IV-1	Affected	4	IV-6	Affected
2	V-1	Affected	5	IV-7	Normal
3	V-3	Affected	6	V-2	Normal
			7	IV-4	Affected

Figure 3.51 Electropherogram of ethidium bromide stained 8% non-denaturing polyacrylamide gel showing allele pattern obtained with marker D1S2660 at 14.75 cM, linked to DFNB36 on chromosome 1p36.3. The Roman with Arabic numerals refers to the individuals in the pedigree.

Family B

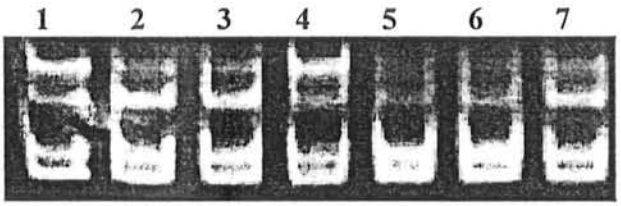

1	IV-1	Affected	4	IV-6	Affected
2	V-1	Affected	5	IV-7	Normal
3	V-3	Affected	6	V-2	Normal
			7	IV-4	Affected

Figure 3.52 Electropherogram of ethidium bromide stained 8% non-denaturing polyacrylamide gel showing allele pattern obtained with marker D11S906 at 88.12 cM, linked to DFNB2 on chromosome 11p13.5. The Roman with Arabic numerals refers to the individuals in the pedigree.

Family B

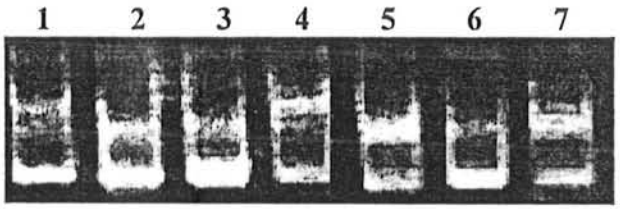

1	IV-1	Affected	4	IV-6	Affected
2	V-1	Affected	5	IV-7	Normal
3	V-3	Affected	6	V-2	Normal
			7	IV-4	Affected

Figure 3.53 Electropherogram of ethidium bromide stained 8% non-denaturing polyacrylamide gel showing allele pattern obtained with marker D11S2002 at 91.48 cM, linked to DFNB2 on chromosome 11p13.5. The Roman with Arabic numerals refers to the individuals in the pedigree.

Family B

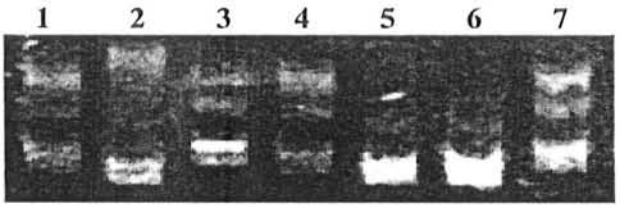

1	IV-1	Affected	4	IV-6	Affected
2	V-1	Affected	5	IV-7	Normal
3	V-3	Affected	6	V-2	Normal
			7	IV-4	Affected

Figure 3.54 Electropherogram of ethidium bromide stained 8% non-denaturing polyacrylamide gel showing allele pattern obtained with marker D17S2196 at 50.99 cM, linked to DFNB3 on chromosome 17p11.2. The Roman with Arabic numerals refers to the individuals in the pedigree.

Family B

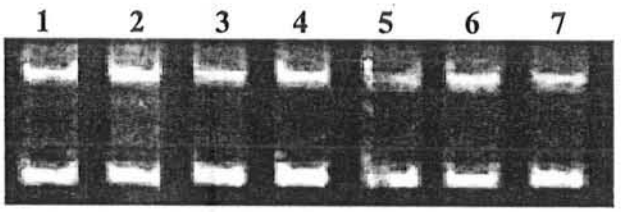

1	IV-1	Affected	4	IV-6	Affected
2	V-1	Affected	5	IV-7	Normal
3	V-3	Affected	6	V-2	Normal
			7	IV-4	Affected

Figure 3.55 Electropherogram of ethidium bromide stained 8% non-denaturing polyacrylamide gel showing allele pattern obtained with marker D17S783 at 54.41 cM, linked to DFNB3 on chromosome 17p11.2. The Roman with Arabic numerals refers to the individuals in the pedigree.

Family B

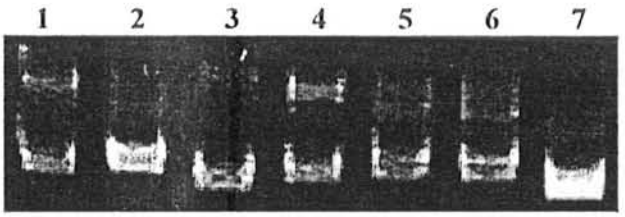

1	IV-1	Affected	4	IV-6	Affected
2	V-1	Affected	5	IV-7	Normal
3	V-3	Affected	6	V-2	Normal
			7	IV-4	Affected

Figure 3.56 Electropherogram of ethidium bromide stained 8% non-denaturing polyacrylamide gel showing allele pattern obtained with marker D7S496 at 117.99 cM, linked to DFNB4 on chromosome 7q31. The Roman with Arabic numerals refers to the individuals in the pedigree.

Family B

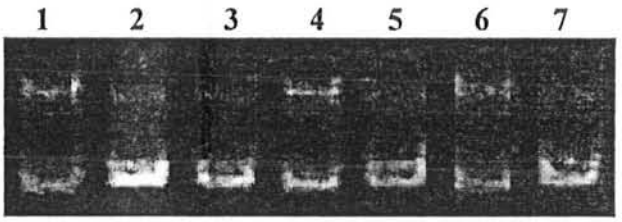

1	IV-1	Affected	4	IV-6	Affected
2	V-1	Affected	5	IV-7	Normal
3	V-3	Affected	6	V-2	Normal
			7	IV-4	Affected

Figure 3.57 Electropherogram of ethidium bromide stained 8% non-denaturing polyacrylamide gel showing allele pattern obtained with marker D7S692 at 119.61 cM, linked to DFNB4 on chromosome 7q31. The Roman with Arabic numerals refers to the individuals in the pedigree.

Family B

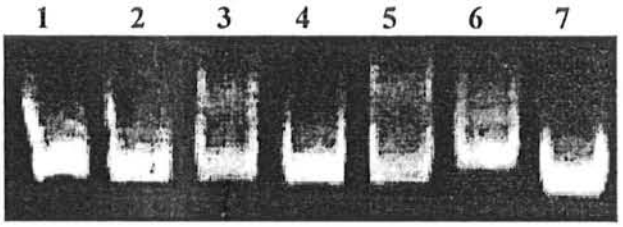

1	IV-1	Affected	4	IV-6	Affected
2	V-1	Affected	5	IV-7	Normal
3	V-3	Affected	6	V-2	Normal
			7	IV-4	Affected

Figure 3.58 Electropherogram of ethidium bromide stained 8% non-denaturing polyacrylamide gel showing allele pattern obtained with marker D21S212 at 58.54 cM, linked to DFNB8 on chromosome 21q22. The Roman with Arabic numerals refers to the individuals in the pedigree.

Family B

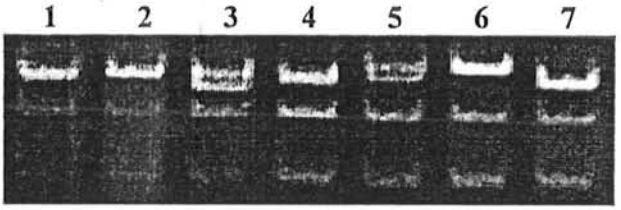

1	IV-1	Affected	4	IV-6	Affected
2	V-1	Affected	5	IV-7	Normal
3	V-3	Affected	6	V-2	Normal
			7	IV-4	Affected

Figure 3.59 Electropherogram of ethidium bromide stained 8% non-denaturing polyacrylamide gel showing allele pattern obtained with marker D21S1411 at 63.83 cM, linked to DFNB8 on chromosome 21q22. The Roman with Arabic numerals refers to the individuals in the pedigree.

Family B

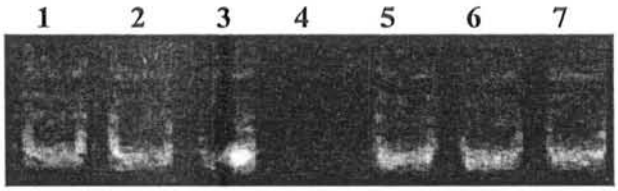

1	IV-1	Affected	4	IV-6	Affected
2	V-1	Affected	5	IV-7	Normal
3	V-3	Affected	6	V-2	Normal
			7	IV-4	Affected

Figure 3.60 Electropherogram of ethidium bromide stained 8% non-denaturing polyacrylamide gel showing allele pattern obtained with marker D10S1688 at 89.34 cM, linked to DFNB12 on chromosome 10q21-22. The Roman with Arabic numerals refers to the individuals in the pedigree.

Family B

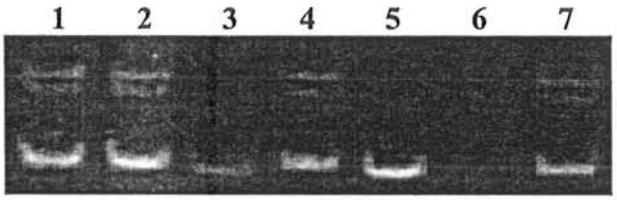

1	IV-1	Affected	4	IV-6	Affected
2	V-1	Affected	5	IV-7	Normal
3	V-3	Affected	6	V-2	Normal
			7	IV-4	Affected

Figure 3.61 Electropherogram of ethidium bromide stained 8% non-denaturing polyacrylamide gel showing allele pattern obtained with marker D10S1432 at 93.70 cM, linked to DFNB12 on chromosome 10q21-22. The Roman with Arabic numerals refers to the individuals in the pedigree.

Family B

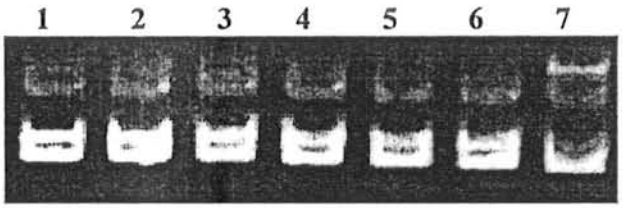

1	IV-1	Affected	4	IV-6	Affected
2	V-1	Affected	5	IV-7	Normal
3	V-3	Affected	6	V-2	Normal
			7	IV-4	Affected

Figure 3.62 Electropherogram of ethidium bromide stained 8% non-denaturing polyacrylamide gel showing allele pattern obtained with marker D15S1044 at 38.97 cM, linked to DFNB16 on chromosome 15q21-22. The Roman with Arabic numerals refers to the individuals in the pedigree.

Family B

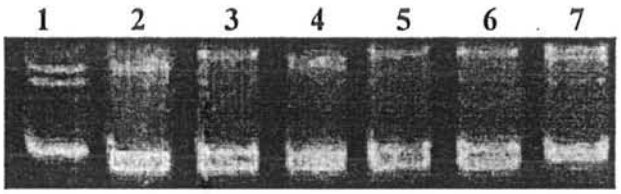

1	IV-1	Affected	4	IV-6	Affected
2	V-1	Affected	5	IV-7	Normal
3	V-3	Affected	6	V-2	Normal
			7	IV-4	Affected

Figure 3.63 Electropherogram of ethidium bromide stained 8% non-denaturing polyacrylamide gel showing allele pattern obtained with marker D15S659 at 43.74 cM, linked to DFNB16 on chromosome 15q21-22. The Roman with Arabic numerals refers to the individuals in the pedigree.

Family B

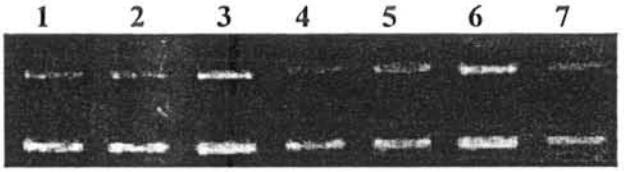

1	IV-1	Affected	4	IV-6	Affected
2	V-1	Affected	5	IV-7	Normal
3	V-3	Affected	6	V-2	Normal
			7	IV-4	Affected

Figure 3.64 Electropherogram of ethidium bromide stained 8% non-denaturing polyacrylamide gel showing allele pattern obtained with marker D11S925 at 130.7 cM, linked to DFNB21 on chromosome 11q. The Roman with Arabic numerals refers to the individuals in the pedigree.

Family B

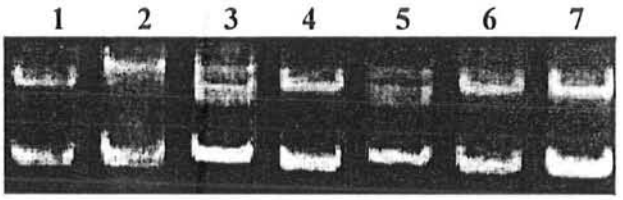

1	IV-1	Affected	4	IV-6	Affected
2	V-1	Affected	5	IV-7	Normal
3	V-3	Affected	6	V-2	Normal
			7	IV-4	Affected

Figure 3.65 Electropherogram of ethidium bromide stained 8% non-denaturing polyacrylamide gel showing allele pattern obtained with marker D11S4464 at 136.99 cM, linked to DFNB21 on chromosome 11q. The Roman with Arabic numerals refers to the individuals in the pedigree.

Family B

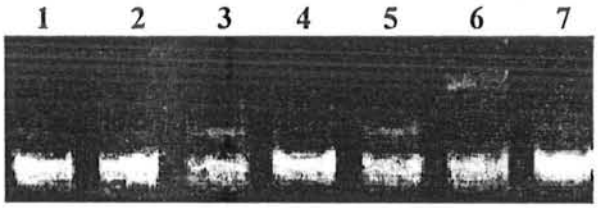

1	IV-1	Affected	4	IV-6	Affected
2	V-1	Affected	5	IV-7	Normal
3	V-3	Affected	6	V-2	Normal
			7	IV-4	Affected

Figure 3.66 Electropherogram of ethidium bromide stained 8% non-denaturing polyacrylamide gel showing allele pattern obtained with marker D21S1440 at 45.42 cM, linked to DFNB29 on chromosome 21q22. The Roman with Arabic numerals refers to the individuals in the pedigree.

Family B

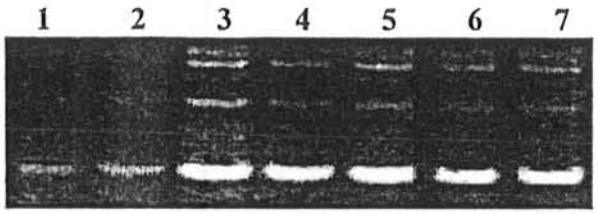

1	IV-1	Affected	4	IV-6	Affected
2	V-1	Affected	5	IV-7	Normal
3	V-3	Affected	6	V-2	Normal
			7	IV-4	Affected

Figure 3.67 Electropherogram of ethidium bromide stained 8% non-denaturing polyacrylamide gel showing allele pattern obtained with marker D21S1246 at 49.49 cM, linked to DFNB29 on chromosome 21q22. The Roman with Arabic numerals refers to the individuals in the pedigree.

Family C

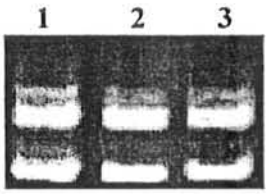

1 IV-1 Normal
2 IV-2 Affected
3 IV-3 Affected

Figure 3.68 Electropherogram of ethidium bromide stained 8% non-denaturing polyacrylamide gel showing allele pattern obtained with marker D13S633 at 2.9 cM, linked to DFNB1 on chromosome 13q12. The Roman with Arabic numerals refers to the individuals in the pedigree.

Family C

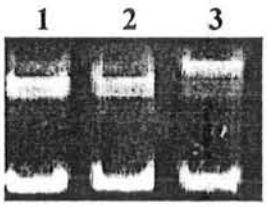

1 IV-1 Normal
2 IV-2 Affected
3 IV-3 Affected

Figure 3.69 Electropherogram of ethidium bromide stained 8% non-denaturing polyacrylamide gel showing allele pattern obtained with marker D13S787 at 8.02 cM, linked to DFNB1 on chromosome 13q12. The Roman with Arabic numerals refers to the individuals in the pedigree.

Family C

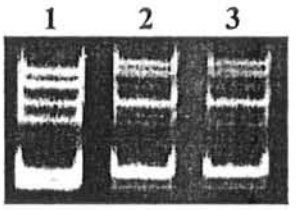

1 IV-1 Normal
2 IV-2 Affected
3 IV-3 Affected

Figure 3.70 Electropherogram of ethidium bromide stained 8% non-denaturing polyacrylamide gel showing allele pattern obtained with marker D5S2500 at 74.39 cM, linked to DFNB49 on chromosome 5q12.3-14.1. The Roman with Arabic numerals refers to the individuals in the pedigree.

Family C

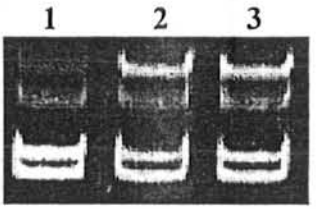

1 IV-1 Normal
2 IV-2 Affected
3 IV-3 Affected

Figure 3.71 Electropherogram of ethidium bromide stained 8% non-denaturing polyacrylamide gel showing allele pattern obtained with marker D5S2003 at 87.39 cM, linked to DFNB49 on chromosome 5q12.3-14.1. The Roman with Arabic numerals refers to the individuals in the pedigree.

Family C

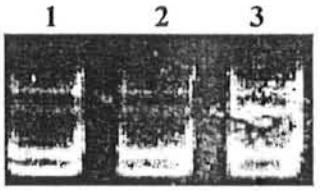

1 IV-1 Normal
2 IV-2 Affected
3 IV-3 Affected

Figure 3.72 Electropherogram of ethidium bromide stained 8% non-denaturing polyacrylamide gel showing allele pattern obtained with marker D11S4120 at 106.3 cM, linked to DFNB24 on chromosome 11q23. The Roman with Arabic numerals refers to the individuals in the pedigree.

Family C

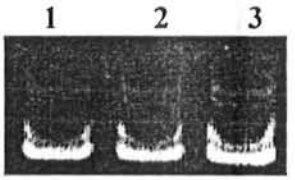

1 IV-1 Normal
2 IV-2 Affected
3 IV-3 Affected

Figure 3.73 Electropherogram of ethidium bromide stained 8% non-denaturing polyacrylamide gel showing allele pattern obtained with marker D11S2017 at 112.89 cM, linked to DFNB24 on chromosome 11q23. The Roman with Arabic numerals refers to the individuals in the pedigree.

Family C

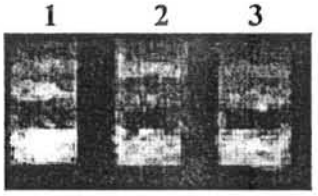

1 IV-1 Normal
2 IV-2 Affected
3 IV-3 Affected

Figure 3.74 Electropherogram of ethidium bromide stained 8% non-denaturing polyacrylamide gel showing allele pattern obtained with marker D3S3647 at 70.02 cM, linked to DFNB6 on chromosome 3p14-21. The Roman with Arabic numerals refers to the individuals in the pedigree.

Family C

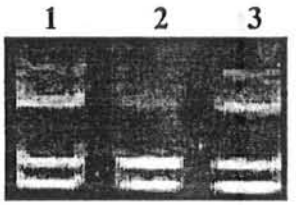

1 IV-1 Normal
2 IV-2 Affected
3 IV-3 Affected

Figure 3.75 Electropherogram of ethidium bromide stained 8% non-denaturing polyacrylamide gel showing allele pattern obtained with marker D3S3582 at 74.08 cM, linked to DFNB6 on chromosome 3p14-21. The Roman with Arabic numerals refers to the individuals in the pedigree.

Family C

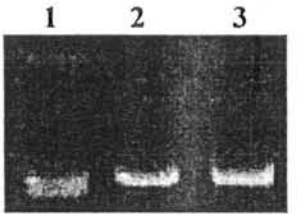

1	IV-1	Normal
2	IV-2	Affected
3	IV-3	Affected

Figure 3.76 Electropherogram of ethidium bromide stained 8% non-denaturing polyacrylamide gel for marker D9S301 at 68.13 cM on chromosome 9p13-21, showing homozygosity among the affected individuals (IV-2, IV-3) of the family 'C'. The Roman with Arabic numerals refers to the individuals in the pedigree.

Family C

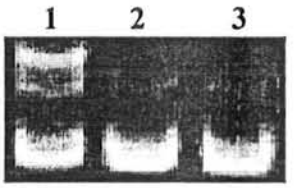

1	IV-1	Normal
2	IV-2	Affected
3	IV-3	Affected

Figure 3.77 Electropherogram of ethidium bromide stained 8% non-denaturing polyacrylamide gel for marker D9S1806 at 68.39 cM on chromosome 9p13-21, showing homozygosity among the affected individuals (IV-2, IV-3) of the family 'C'. The Roman with Arabic numerals refers to the individuals in the pedigree.

Family C

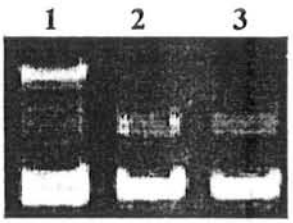

1 IV-1 Normal
2 IV-2 Affected
3 IV-3 Affected

Figure 3.78 Electropherogram of ethidium bromide stained 8% non-denaturing polyacrylamide gel for marker D9S1876 at 69.4 cM on chromosome 9p13-21, showing homozygosity among the affected individuals (IV-2, IV-3) of the family 'C'. The Roman with Arabic numerals refers to the individuals in the pedigree.

Family C

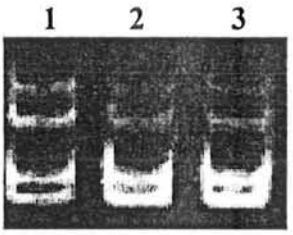

1 IV-1 Normal
2 IV-2 Affected
3 IV-3 Affected

Figure 3.79 Electropherogram of ethidium bromide stained 8% non-denaturing polyacrylamide gel for marker D9S175 at 71.93 cM on chromosome 9p13-21, showing homozygosity among the affected individuals (IV-2, IV-3) of the family 'C'. The Roman with Arabic numerals refers to the individuals in the pedigree.

Discussion

DISCUSSION

Hearing loss is a complete or partial decrease in the ability to detect or understand sound. Loss of hearing can occur to any organism that can perceive sound. The incidence of congenital hearing loss is estimated at 1 in 1000 births, of which approximately equal numbers of cases are attributed to environmental and genetic factors (Morton, 1991).

After 1995, when first gene for hearing loss was identified, a great number of new genes have been characterized to date for hearing loss. Moreover, the elucidation of the exact function of genes for which only a putative function was proposed, and of genes with an unknown function remains a great challenge (Francis *et al.*, 2004).

Environmental factors leading to hearing loss include acoustic trauma, ototoxic drugs, and bacterial and viral infections. Of the hearing loss disorders attributable to genetic caused ~70% are classified as nonsyndromic in which there are no additional abnormalities and the remaining 30% are syndromic, in which deafness is accompanied by other specific abnormalities.

Nonsyndromic hearing impairment can be further subdivided by mode of inheritance: 77% of cases are autosomal recessive, 20% are autosomal dominant, 1% is X-linked and < 1% is due to mitochondrial inheritance (Morton *et al.*, 1991). Approximately 120 different gene loci associated with nonsyndromic hearing impairment have been identified. Presently 54 gene loci associated with autosomal dominant mode of inheritance and 71 gene loci with autosomal recessive mode of inheritance have been identified, 7 are X-linked and 4 mitochondrial.

Among the many disorders classified as syndromic hearing loss, the pathology varies widely, but in nonsyndromic deafness, the defect is generally sensorineural. Severe to profound hearing impairment with onset before 12 month of age (prelingual) is a characteristic of the affected individuals of most of the families for which gene causing recessive hearing impairment have localized.

These genes encode proteins of diverse functions including transcription factors, cytoskeletal and extra cellular matrix components and ion channels (Birkenhager *et al.*, 2007). Despite this heterogeneity, up to 50% of prelingual recessive nonsyndromic deafness can be attributed to mutation in the *GJB2* (connexin-26, gap-junction protein).

However the diversity of genes and genetic loci implicated in hearing loss illustrates the complexity of the genetic bases of hearing.

In the present study, three highly consanguineous families A, B, and C demonstrating autosomal recessive form of nonsyndromic deafness was ascertained. The affected individuals in the families had prelingual severe to profound hearing loss with no associated features of syndromic or acquired form of deafness. The affected individuals from various age groups showed the same level of sever hearing loss implying that deafness was not progressive in any of the families studied.

Genetic linkage analysis is a statistical technique used to map the disease genes. Linkage analysis is a relationship between the loci and two loci on the same chromosome are said to be linked if the phenomenon of crossing over does not separate them. The most common application of linkage analysis is to try and find the location, in the genome, of a gene responsible for a certain mendelianly-inherited disease (Ott, 1985). Alleles at loci on same chromosome should co-segregate at a rate that is somehow related to the distance between them on the chromosome. This rate is the probability or recombination fraction (0), of a recombination event occurring between two loci. Two loci are said to be genetically linked when recombination fraction is less than 0.5. The objective of linkage analysis is to estimate recombination fraction and to test if θ is less than 0.5 between two loci i.e. whether an observed deviation from 50% recombination is statistically significant.

To identify the causative genes underlying hereditary hearing loss in the families presented here, a classical linkage analysis approach called "Homozygosity Mapping" was followed. Smith, (1953) indicated that offspring of consanguineous matings are homozygous for genetic markers located near the disease gene. Lander and Botstein, (1987) reasoned that a recessive gene could be mapped using the offspring of consanguineous unions in an approach they called "Homozygosity Mapping", which provides a rapid mean of mapping autosomal recessive genes in consanguineous families by identifying chromosomal regions that show homozygous identity-by-descend (IBD) segments in pooled samples (Miano *et al.*, 2000). In affected children of such union, a region of many centi-Morgans (cM) spanning the disease locus is almost always homozygous by descent. Other regions also will be homozygous by descent, but these

regions will vary from one child to the next. The homozygosity mapping revolves around the identification/detection of this homozygous region among all the affected individuals. The minimum detectable length of a homozygous segment depends on marker density of screening set and their heterozygosity. For markers with 70% heterozygosity, a homozygous segment as short as 9 cM may be detected when the markers are 1 cM apart. This may suggest that with the density of a genome scan of 20 cM, only very large homozygous segments can be detected (Broman and Weber, 1999).

Although the prevalence of *GJB2* mutations in Pakistani deaf families is low as compared to other population, they are the most common cause of autosomal recessive nonsyndromic deafness world wide (Santos *et al.*, 2005). Therefore the coding exon of *GJB2* gene was sequenced in affected individual of family 'A' but no sequence variant was observed. The family 'A' was then tested for mapping to other known loci by using microsatellite markers from their candidate linkage intervals. Electorpherogram obtained by genotyping the markers revealed that the affected individuals were heterozygous for different combinations of parental alleles, thus excluding family 'A' from linkage to known loci (Figures 3.4-3.35)

Family 'B' was also tested for linkage to several known loci by suing polymorphic microsatellite markers from their candidate linkage intervals. Linkage to DFNB1 (Figure 3.36, 3.37) was also checked by sequencing the coding region of exon 2 of *GJB2* gene. Electorpherogram obtained by genotyping the markers revealed that the affected individuals were heterozygous for different combination of parental alleles, thus excluding family 'B' form linkage to known loci (Figures 3.38-3.67)

In family 'C' linkage was detected to DFNB7/11 locus on chromosome 9q13-21, where candidate gene is *TMC1* (Figure 3.76-3.80). By alignment of the *TMC1* cDNA with genomic sequences, Kurima et al. (2002) showed that 24 exons probably encode full-length mRNA, including 4 exons encoding sequence upstream of a methionine codon in exon 5. There are many in-frame stop codons directly upstream of this methionine codon, which was predicted to be an adequate Kozak translation initiation codon. The candidate gene, *TMC1* within linkage interval of 3.80 Mb was screened in an affected individual. Sequence analysis of all the 24 exons and splice junctions of TMC1 gene failed to

identify any functional sequence variant. Therefore, it is possible that the mutation is located in the regulatory parts of *TMC1* gene.

Up till now total 9 different *TMC1* mutations have been reported in different populations of the world. (Kitajiri *et al.*, 2007). Kurima *et al.* (2002) found that 5 different families from Pakistan with autosomal recessive, nonsyndromic deafness had a 100C>T transition in the *TMC1* gene resulting in an arg34-ter (R34X) nonsense mutation and a family had a 1960A>G transition in *TMC1* gene predicted to substitute valine for conserved methionine at position 654 (M654V). Mayer *et al.* (2005) have identified the structural variant 1165C>T in exon 13 of *TMC1* leading to stop codon arg389X and the splice-site variant 19+5G>A, independently segregating with in the deafness phenotypes. Santos *et al.* (2005) have reported the identification of five novel but putatively functional nonsyndromic sequence variants, 830A>G, 1114G>A, 1334G>A, 2004T>G and 2035G>A in the *TMC1* gene (MIM 606706), located at DFNB7/11 locus. The *TMC1* protein is predicted to contain six transmembrane domains and have cytoplasmic orientation of N and C termini. Kurima *et al.* (2002) found that largest open reading frame to be 2283 nucleotides predicting an 87 kDa protein. The mouse *Tmc1* mRNA is expressed in hair cells of the postnatal cochlea and vestibular end organs and is required for normal functioning of cochlear hair cells.

References

REFERENCES

Ahmad ZM, Riazuddin S, Ahmad J, Bernstein SL, Guo Y, Sabar MF, Sieving P, Riazuddin S, Griffith AJ, Friedman TB, Belyantseva IA, Wilcox ER (2003). *PCDH15* is expressed in the neurosensory epithelium of the eye and ear and mutant alleles are responsible for both USH1F and DFNB23. Hum Mol Genet 12: 3215–3223.

Ahmed ZM, Riazuddin S, Bernstein SL, Ahmed Z, Khan S, Griffith AJ, Morell RJ, Friedman TB, Riazuddin S, Wilcox ER (2001). Mutations of the protocadherin gene *PCDH15* cause Usher syndrome type 1F. Am J Hum Genet 69: 25–34.

Alagramam KN, Murcia CL, Kwon HY, Pawlowski KS, Wright CG, Woychik RP (2001). The mouse Ames waltzer hearing-loss mutant is caused by mutation of *Pcdh15*, a novel protocadherin gene. Nat Genet 27: 99–102.

Anderson DW, Probst FJ, Belyantseva IA, Fridell RA, Beyer L, Martin DM, Wu D, Kachar B, Friedman TB, Raphael Y, Camper SA (2000). The motor and tail regions of myosin XV are critical for normal structure and function of auditory and vestibular hair cells. Hum Mol Genet 9: 1729–1738.

Beighton P (1983). Hereditary deafness. In Emery AEH, Rimoin DL, eds. Principles and Practive of Medical Genetics. Churchill Livingstone, New York: 562-575.

Ben-Yosef T, Belyantseva IA, Saunders TL, Hughes ED, Kawamoto K, Van Itallie CM, Beyer LA, Halsey K, Gardner DJ, Wilcox ER, Rasmussen J, Anderson JM, Dolan DF, Forge A, Raphael Y, Camper SA, Friedman TB (2003). Claudin 14 knockout mice, a model for autosomal recessive deafness DFNB29, are deaf due to cochlear hair cell degeneration. Hum Mol Genet 12: 2049–2061.

Birkenhager R, Aschendorff A, Schipper J, Laszig R (2007). Non-syndromic hereditary hearing impairment 86: 299-309.

Broman KW, Weber JL (1999). Long homozygous chromosomal segments in reference families from the Centre d'Etude du polymorphisme Humain. Am J Hum Genet 65: 1493-1500.

Campbell C, Cucci RA, Prasad S, Green GE, Edeal JB, Galer CE, Karniski LP, Sheffield VC, Smith RJ. Pendred syndrome, DFNB4, and *PDS/SLC26A4* (2001).

Identification of eight novel mutations and possible genotype-phenotype correlations. Hum Mutat 17: 403–411.

Chaib H, Place C, Salem N, Chardenoux S, Vincent C, Weissenbach J, el Zir E, Loiselet J, Petit C (1996). A gene responsible for a sensorineural nonsyndromic recessive deafness maps to chromosome 2p22-23. Hum Mol Gent 5: 155-158.

Cheney RE, Riley MA, Mooseker MS (1993). Phylogenetic analysis of the myosin superfamily. Cell Motil Cytoskeleton 24: 215-223.

Cremers CW, Beusen JM, Huygen PL (1991). Hearing gain after stapedotomy, partial platinectomy, or total stapedectomy for otosclerosis. Ann Otol Rhinol Laryngol 100: 959-961.

Davis A, Parving A (1994). Towards appropriate epidemiology data on childhood hearing disability: a comparative European study of birth-cohorts 1982-1988. J Audiol Med Genet 46: 486-491.

Denoyelle F, Weil D, Maw MA (1997). Prelingual deafness: high prevalence of a 30delG mutation in the connexin 26 gene. Hum Mol Genet 6: 2173–2177.

Di Palma F, Holme RH, Bryda EC, Belyantseva IA, Pellegrino R, Kachar B, Steel KP, Noben-Trauth K (2001). Mutations in *Cdh23,* encoding a new type of cadherin, cause stereocilia disorganization in waltzer, the mouse model for Ushersyndrome type 1D. Nat Genet 27: 103–107.

Dose AC, Burnside B (2000). Cloning and chromosomal localization of a human class III myosin. Genomics 67: 333–342.

Estivill X, Fortina P, Surrey S (1998). Connexin-26 mutations in sporadic and inherited sensorineural deafness. Lancet 351: 394–398.

Friedman TB, Griffith AJ (2003). Human nonsyndromic sensorineural deafness. Ann Rev Genomics Hum Genet 4: 341-402.

Fukushima K, Ramesh A, Srisailapathy CRS Ni L, Wayne S, O'Neil ME, Van Camp G, Coucke P, Jain P, Wilcox ER (1995). An autosomal recessive non-syndromic form of sensorineural hearing loss maps to 3p-DFNB6. Genome Res 5: 305–308.

Gorlin JB, Wengler G, Williamson JM, Rosen FS, Bing DH (1995). Nonrandom inactivation of the X chromosome in early lineage hematopoietic cells in carriers of Wiskott-Aldrich syndrome. Blood Genomics 85: 2471-2477.

Grifa A, Wagner CA, D'Ambrosio L, Melchionda S, Bernardi F, Lopez-Bigas N, Rabionet R, Arbones M, Monica MD, Estivill X, Zelante L, Lang F, Gasparini P (1999). Mutations in *GJB6* cause nonsyndromic autosomal dominant deafness at DFNA3 locus. Nat Genet 23:16–18.

Guilford P, Ayadi H, Blanchard S, Chaib H, Le Paslier D (1994). A human gene responsible for neurosensory, nonsyndromic recessive deafness is a candidate homologue of the mouse sh-1 gene. Hum Mol Genet 3: 989-993.

Guipponi M, Vuagniaux G, Wattenhofer M, Shibuya K, Vazquez M, Dougherty L, Scamuffa N, Guida E, Okui M, Rossier C, Hancock M, Buchet K, Reymond A, Hummler E, Marzella PL, Kudoh J, Shimizu N, Scott HS, Antonarakis SE, Rossier BC (2002). The transmembrane serine protease (*TMPRSS3*) mutated in deafness DFNB8/10 activates the epithelial sodium channel (ENaC) in vitro. Hum Mol Genet 11: 2829–2836.

Harris S, Casselbrant M, Ivarsson A, Tjernstrom O (1984). Hearing threshold measurement in Meniere's disease. Audiology 23: 46-52.

Hicks T, Fowler K, Richardson M, Dahle A, Adams L, Pass R (1993). Congenital cytomegalovirus infection and neonatal auditory screening. J Pediatr 123: 779-782.

Holt JR, Corey DP (1999). Ion channel defects in hereditary hearing loss. Neuron 22: 217-219.

Hudspeth AJ (1997). How hearing happens. Neuron 19: 947-950.

Janecke AR, Meins M, Sadeghi M, Grundmann K, Apfelstedt-Sylla E, Zrenner E, Rosenberg T, Gal A (1999). Twelve novel myosin *VIIA* mutations in 34 patients with Usher syndrome type I. confirmation of genetic heterogeneity. Hum Mutat 13: 133–140.

John FB, Matthew AH (2002). Hearing, Chapter in encyclopedia of the Human Brain. Elsevier: 429-448.

Kelley PM, Harris DJ, Comer BC, Askew JW, Fowler T, Smith SD, Kimberling WJ (1998). Novel mutations in the connexin26 gene (*GJB2*) hearing loss. Am J Hum Genet 62: 792-799.

Kelsell DP, Dunlop J, Steven HP, Lench NJ, Liang J, Parry G, Muller RF, Leigh IM (1997). Connexin 26 mutations in hereditary nonsyndromic sensorineural deafness. Nature 387: 80-83.

Kikkawa Y, Mburu P, Morse S, Kominami R, Townsend S, Brown SD (2005). Mutant analysis reveals whirlin as a dynamic organizer in the growing hair cell stereocilium. Hum Mol Genet 14: 391–400.

Kitajiri SI, McNamara R, Makishima T, Husnain T, Zafar A, Kittles R, Ahmad Z, Friedman T, Riazuddin S, Griffieth D (2007). Identities, frequencies and origins of *TMC1* mutations causing DFNB7/B11 deafness in Pakistan. Clin Genet: Epub ahead of print.

Kumar NM, Gilula NB (1996). The gap junction communication channel. Cell 84: 381-388.

Kurima K, Peters LM, Yang Y, Riazuddin S, Ahmed ZM, Naz S, Arnaud D, Drury S, Mo J, Makishima T, Ghosh M, Menon PS, Deshmukh D, Oddoux C, Ostrer H, Khan S, Riazuddin S, Deininger PL, Hampton LL, Sullivan SL, Battey JF Jr, Keats BJ, Wilcox ER, Friedman TB, Griffith AJ (2002). Dominant and recessive deafness caused by mutations of a novel gene, *TMC1*, required for cochlear hair-cell function. Nat Genet30: 277–284.

Lamartine J, Munhoz Essenfelder G, Kibar Z, Lanneluc I, Callouet E, Laoudj D, Lemaitre G, Hand C, Hayflick SJ, Zonana J, Antonarakis S, Radhakrishna U, Kelsell DP, Christianson AL, Pitaval A, Der Kaloustian V, Fraser C, Blanchet-Bardon C, Rouleau GA, Waksman G (2000). Mutations in *GJB6* cause hidrotic ectodermal dysplasia. Nat Genet 26:142–144.

Lander ES, Botstein D (1987). Homozygosity mapping: a way to map human recessive traits with the DNA of inbred children. Science 236: 1567-1570.

Legan PK, Lukashkina VA, Goodyear RJ, Kossi M, Russell IJ, Richardson GP (2000). A targeted deletion in alpha-tectorin reveals that the tectorial membrane is required for the gain and timing of cochlear feedback. Neuron 28: 273–285.

Marazita ML, Ploughman LM, Rawlings B, Remington E, Arnos KS, Nance WE (1993). Genetic epidemiological studies of early-onset deafness in the U.S. school-age population. Am J Med Genet 46: 486-491.

Mburu P, Mustapha M, Varela A, Weil D, El-Amraoui A, Holme RH, Rump A, Hardisty RE, Blanchard S, Coimbra RS, Perfettini I, Parkinson N, Mallon AM, Glenister P, Rogers MJ, Paige AJ, Moir L, Clay J, Rosenthal A, Liu XZ, Blanco G, Steel KP, Petit C, Brown SD (2003). Defects in whirlin, a PDZ domain molecule involved in stereocilia elongation, cause deafness in the whirler mouse and families with DFNB31. Nat Genet 34: 421–428.

Meyer CG, Gasmelseed NM, Mergani A, Magzonb MM, Muntau B, Thye T, Grostmanm D (2005). Novel *TMC1* structural and splice variants associated with congenitall nonsyndromic deafness in a Sudanese pedigree. Hum Mutat 25: 100-110.

Miano MG, Jacobson SG, Carothers A, Hanson I, Teague P, Lovell J, Cideciyan AV, Haider N, Stone EM, Sheffield VC, Wright AF (2000). Pitfalls in homozygosity mapping. Am J Hum Genet 67: 1348-1351.

Mooseker MS, Cheney RE (1995). Unconventional myosins. Annu Rev Cell Dev Biol 11: 633-675.

Morton NE (1991). Genetic epidemiology of hearing impairment. Ann N Y Acad Sci 630: 16-31.

Naz S, Giguere CM, Kohrman DC, Mitchem KL, Riazuddin S, Morell RJ, Ramesh A, Srisailpathy S, Deshmukh D, Riazuddin S, Griffith AJ, Friedman TB, Smith RJ, Wilcox ER (2002). Mutations in a novel gene, *TMIE*, are associated with hearing loss linked to the DFNB6 locus. Am J Hum Genet 71: 632–636.

Naz S, Griffith AJ, Riazuddin S, Hampton LL, Battey JF Jr, Khan SN, Riazuddin S, Wilcox ER, Friedman TB (2004). Mutations of *ESPN* cause autosomal recessive deafness and vestibular dysfunction. J Med Genet 41: 591–595.

Ott J (1985). A chi-square test to distinguish allelic association from other causes of phenotypic association between two loci. Genet Epidemiol 2: 79-84.

Petit C, Levilliers J, Hardelin J-P (2001). Molecular Genetics of hearing loss. Ann Rev Genet 35: 589-646.

Probst FJ, Fridell RA, Raphael Y, Saunders TL, Wang A, Liang Y, Morell RJ, Touchman JW, Lyons RH, Noben-Trauth K, Friedman TB, Camper SA (1998). Correction of deafness in shaker-2 mice by an unconventional myosin in a BAC transgene. Science 280: 1444–1447.

Ramzan K, Shaikh RS, Ahmad J, Khan SN, Riazuddin S, Ahmed ZM, Friedman TB, Wilcox ER, Riazuddin S (2005). A new locus for nonsyndromic deafness DFNB49 maps to chromosome 5q12.3-q14.1. Hum Genet 116: 17-22.

Resendes BL, Williamson RE, Morton CC (2001). Gene discovery in the auditory system. Am J Hum Genet 69: 923-935.

Riazuddin S, Ahmed ZM, Fanning AS, Lagziel A, Kitajiri S, Ramzan K, Khan SN, Chattaraj P, Friedman PL, Anderson JM, Belyantseva IA, Forge A, Riazuddin S, Friedman TB (2006). Tricellulin is a tight-junction protein necessary for hearing. Am J Hum Genet 79: 1040-1051.

Santos RL, Wajid M, Khan MN, McArthur N, Pham TL, Bhatti A, Lee K, Irshad S, Mir A, Yan K, Chahrour MH, Ansar M, Ahmad W, Leal SM (2005). Novel sequence variants in the *TMC1* gene in Pakistani families with autosomal recessive hearing impairment. Hum Mutat 4: 396-404.

Schrijver I (2004). Hereditary non-syndromic sensorineural hearing loss. J Mol Diagnost 6: 275-284.

Scott DA, Wang R, Kreman TM, Andrews M, McDonald JM, Bishop JR, Smith RJ, Karniski LP, Sheffield VC (2001). Functional differences of the *PDS* gene product are associated with phenotypic variation in patients with Pendred syndrome and non-syndromic hearing loss (DFNB4). Hum Mol Genet 9: 1709–1715.

Scott HS, Kudoh J, Wattenhofer M, Shibuya K, Berry A, Chrast R, Guipponi M, Wang J, Kawasaki K, Asakawa S, Minoshima S, Younus F, Mehdi SQ, Radhakrishna U, Papasavvas MP, Gehrig C, Rossier C, Korostishevsky M, Gal A, Shimizu N, Bonne-Tamir B, Antonarakis SE (2001). Insertion of ß-satellite repeats identifies a transmembrane protease causing both congenital and childhood onset autosomal resessive deafness. Nat Genet 27: 59–63.

Siemens J, Kazmierczak P, Reynolds A, Sticker M, Littlewood-Evans A, Muller U (2002). The Usher syndrome proteins cadherin 23 and harmonin form a complex by means of PDZ–domain interactions. Proc Natl Acad Sci USA 99: 14946–14951.

Siemens J, Lillo C, Dumont RA, Reynolds A, Williams DS, Gillespie PG, Muller U (2004). Cadherin 23 is a component of the tip link in hair-cell stereocilia. Nature 428: 950–954.

Smith FJ, Morley SM, McLean WH (2002). A novel connexin 30 mutation in Clouston syndrome. J Invest Dermatol 118: 530-532.

Steel KP, Corey DP (1999). The benefits of recycling. Science 285: 1363-1364.

Steel KP, Kros CJ (2001). A genetic approach to understanding auditory function. Nat Genet 27: 143-149.

Tekin M, Akcayoz D, Incesulu A (2005). A novel missense mutation in a C2 domain of *OTOF* results in autosomal recessive auditory neuropathy. Am J Med Genet 138: 6–10.

Tsukita S, Furuse M (2000). The structure and function of claudins, cell adhesion molecules at tight junctions. Ann N Y Acad Sci 915: 129–135.

Van Camp G, Willems PJ, Smith RJ (1997). Non-syndromic hearing impairment: unparalleled heterogeneity. Am J Hum Genet 60: 758-764.

Varga R, Kelley PM, Keats BJ, Starr A, Leal SM, Cohn E, Kimberling WJ (2003). Non-syndromic recessive auditory neuropathy is the result of mutations in the otoferlin (*OTOF*) gene. J Med Genet 40: 45–50.

Verpy E, Leibovici M, Zwaenepoel I, Liu XZ, Gal A, Salem N, Mansour A, Blanchard S, Kobayashi I, Keats BJ, Slim R, Petit C (2000). A defect in harmonin, a PDZ domain-containing protein expressed in the inner ear sensory hair cells, underlies Usher syndrome type 1C. Nat Genet 26: 51–55.

Verpy E, Masmoudi S, Zwaenepoel I, Leibovici M, Hutchin TP, Del Castillo I, Nouaille S, Blanchard S, Laine S, Popot JL, Moreno F, Mueller RF, Petit C (2001). Mutations in a new gene encoding a protein of the hair bundle cause nonsyndromic deafness at the DFNB16 locus. Nat Genet 29: 345–349.

Walsh T, Walsh V, Vreugde S, Hertzano R, Shahin H, Haika S, Lee MK, Kanaan M, King MC, Avraham KB (2002). From flies' eyes to our ears: mutations in a human class III myosin cause progressive nonsyndromic hearing loss DFNB30. Proc Natl Acad Sci USA 99: 7518–7523.

Weil D, Blanchard S, Kaplan J, Guilford P, Gibson F, Walsh J, Mburu P, Varela A, Levilliers J, Weston MD (1995). Defective myosin *VIIA* gene responsible for Usher syndrome type 1B. Nature 374: 60-61.

Weil D, Kussel P, Blanchard S, Levy G, Levi-Acobas F, Drira M, Ayadi H, Petit C (1997). The autosomal recessive isolated deafness, DFNB2, and the Usher 1B syndrome are allelic defects of the myosin-*VIIA* gene. Nat Genet 16: 191-193.

Weil W, Levy G, Sahly I, Levi-Acobas F, Blanchard S, El-Amraoui A, Crozet F, Philippe H, Abitbol M, Petit C (1996). Human myosin *VIIA* responsible for the Usher 1B syndrome: a predicted membrane-associated motor protein expressed in developing sensory epithelia. Proc Natl Acad Sci USA 93: 3232–3237.

Wright G, Davis A, Bredberg G, Ulehlova L, Spencer H, Bock G, Felix H, Lurato S, Johnsoon LG, Pauler M (1987). Acta Otolaryngol Suppl 444: 1-48.

Yasunaga S, Grati M, Chardenoux S, Smith TN, Friedman TB, Lalwani AK, Wilcox ER, Petit C (2000). *OTOF* encodes multiple long and short isoforms: genetic evidence that the long ones underlie recessive deafness DFNB9. Am J Hum Genet 67: 591–600.

Yasunaga S, Grati M, Cohen-Salmon M, El-Amraoui A, Mustapha M, Salem N, El-Zir E, Loiselet J, Petit C (1999). A mutation in *OTOF*, encoding otoferlin, a FER-1-like protein, causes DFNB9, a nonsyndromic form of deafness. Nat Genet 21: 363–369.

Zelante L, Gasparini P, Estivill X, Melchionda S, D'Agruma L, Govea N, Mila M, Monica MD, Lutfi J, Shohat M, Mansfield E, Delgrosso K, Rappaport E, Surrey S, Fortina P (1997). Connexin26 mutations associated with the most common form of nonsyndromic neurosensory autosomal recessive deafness (DFNB1) in Mediterraneans. Hum Mol Genet 6: 1605-1609.

Zheng L, Sekerkova G, Vranich K, Tilney LG, Mugnaini E, Bartles JR (2000). The deaf jerker mouse has a mutation in the gene encoding the espin actinbundling proteins of hair cell stereocilia and lacks espins. Cell 102: 377–385.

Zwaenepoel I, Mustapha M, Leibovici M, Verpy E, Goodyear R, Liu XZ, Nouaille S, Nance WE, Kanaan M, Avraham KB, Tekaia F, Loiselet J, Lathrop M, Richardson G, Petit C (2002). Otoancorin, an inner ear protein restricted to the

interface between the apical surface of sensory epithelia and their overlying acellular gels, is defective in autosomal recessive deafness DFNB22. Proc Natl Acad Sci USA 99: 6240–6245.

Electronic Database Information

- Deafness and Hereditary Hearing loss overview.
  URL: http://www.geneclinics.org/servlet
- Ensemble Genome Browser.
  URL: http://www.ensemble.org/index.html
- Genome Database Homepage.
  URL: http://www.gdb.org
- Hereditary Hearing Loss Homepage.
  URL: http://dnalab-www.uia.ac.be/dnalab/hhh
- Human Gene Mutation Database.
  URL: http://www.hgmd.org
- Online Mendelian Inheritance in Man.
  URL: http://www.ncbi.nlm.nih.gov